Ovariectomy Augments Hypertension Through Rho-Kinase Activation in the Brain Stem in Female Spontaneously Hypertensive Rats

Koji Ito, Yoshitaka Hirooka, Yoshikuni Kimura, Yoji Sagara, Kenji Sunagawa

Abstract—Estrogen protects against increases in arterial pressure (AP) by acting on blood vessels and on cardiovascular centers in the brain. The mechanisms underlying the effects of estrogen in the brain stem, however, are not clear. The aim of the present study was to determine whether ovariectomy affects AP via the Rho/Rho-kinase pathway in the brain stem. We performed bilateral ovariectomy in 12-week-old female spontaneously hypertensive rats. AP and heart rate (HR), measured using radiotelemetry in awake rats, were increased in ovariectomized rats compared with control rats (mean AP: 163±3 versus 144±4 mm Hg; HR: 455±4 versus 380±6 bpm). Continuous intracisternal infusion of Y-27632 significantly attenuated the ovariectomy-induced increase in AP and HR (mean AP: 137±6 versus 163±3 mm Hg; HR: 379±10 versus 455±4 bpm). In addition, we confirmed the increase of Rho-kinase activity in the brain stem in ovariectomized rats, and the increase was attenuated by intracisternal infusion of Y-27632 via the phosphorylated ezrin, radixin, and moesin (ERM) family, which are Rho-kinase target proteins. Furthermore, angiotensin II type 1 receptor expression in the brain stem was significantly greater in ovariectomized rats than in control rats, and the increase was partially reduced by intracisternal infusion of Y-27632. In a separate group of animals, we confirmed that the serum and cerebrospinal fluid 17β-estradiol concentrations decreased in ovariectomized rats. These results suggest that depletion of endogenous estrogen by ovariectomy, at least in part, induces hypertension in female spontaneously hypertensive rats via activation of the renin–angiotensin system and the Rho/Rho-kinase pathway in the brain stem. (***Hypertension*. 2006;48:651-657.**)

Key Words: estrogen ■ brain ■ nervous system, sympathetic ■ receptors, angiotensin ■ blood pressure ■ heart rate

The incidence of cardiovascular diseases is lower in premenopausal women than in age-matched men[1–3] and postmenopausal women.[4] The decreased protective effect against cardiovascular diseases, such as hypertension, in postmenopausal women is thought to be because of endogenous ovarian estrogen depletion. Estrogen decreases arterial pressure through direct effects on blood vessels[5,6] and through effects on central cardiovascular regulatory centers by modulating autonomic function of the cardiovascular system.[7,8] Hormone replacement therapy in postmenopausal women favorably affects cardiovascular regulation by improving baroreflex function and heart rate (HR) variability (HRV)[8] and by decreasing sympathetic nerve activity.[9] In the central nervous system (CNS), endogenous estrogen has numerous effects through estrogen receptor–dependent and -independent pathways.[10,11] Estrogen and estrogen receptors are present in the brain stem where the vasomotor centers, such as the nucleus tractus solitarius (NTS) and the ventrolateral medulla, are located.[12] Medullary injections of exogenous estrogen decrease arterial pressure, HR, and renal sympathetic nerve activity and enhance reflex control of the HR in male rats, as well as in ovariectomized female rats,[13] suggesting that estrogen has beneficial effects on autonomic functions.[14]

Rho-Kinase is a serine–threonine protein kinase and is one of the effectors of the small GTP-binding protein Rho. This pathway is involved in various cellular functions including smooth muscle contraction, actin cytoskeleton organization, cell proliferation, and cell motility.[15–18] In vascular smooth muscle cells, activation of this pathway contributes to the pathophysiology of hypertension via smooth muscle contraction.[19,20] In the CNS, the Rho/Rho-kinase pathway contributes to the formation of dendritic spines.[21] Dendritic spines form the postsynaptic contact sites of excitatory synapses in the CNS[22] and are thought to be involved in synaptic transmission.[23] We reported previously that Rho-kinase in the brain stem modulates glutamate sensitivity[24] and maintains arterial pressure via the sympathetic nervous system and that activation of the Rho/Rho-kinase pathway might contribute to the central mechanisms of hypertension.[25,26] Estrogen also regulates the formation of excitatory synapses on dendritic spines.[27] Estrogen treatment increases spine number and

Received January 18, 2006; first decision February 6, 2006; revision accepted July 18, 2006.

From the Department of Cardiovascular Medicine, Kyushu University Graduate School of Medical Sciences, Fukuoka, Japan.

Correspondence to Yoshitaka Hirooka, Department of Cardiovascular Medicine, Kyushu University Graduate School of Medical Sciences, 3-1-1 Maidashi, Higashi-ku, Fukuoka 812-8582, Japan. E-mail hyoshi@cardiol.med.kyushu-u.ac.jp

Hypertension **is available at http://www.hypertensionaha.org** **DOI: 10.1161/01.HYP.0000238125.21656.9e**

synaptic density on apical and basal dendrites of CA1 pyramidal neurons in ovariectomized adult female rats.[28,29] These findings led to the hypothesis that the effects of endogenous estrogen on central cardiovascular regulation involve alterations in Rho-kinase activity in the central cardiovascular center. Therefore, the aim of the present study was to determine whether the depletion of endogenous estrogen affects arterial pressure via the Rho/Rho-kinase pathway in the brain stem.

For this purpose, we performed a bilateral ovariectomy in 12-week-old female spontaneously hypertensive rats (SHRs). Y-27632, a specific Rho-kinase inhibitor,[30] was then infused intracisternally for 2 weeks with a miniosmotic pump. Arterial pressure and HR were measured in awake rats using a radiotelemetry system.[31] In a separate group of animals, we confirmed that serum and cerebrospinal fluid (CSF) 17β-estradiol concentrations were decreased in ovariectomized rats. We then compared the Rho-kinase activity in the brain stem between control rats and ovariectomized rats. Finally, we compared the expression level of angiotensin II type 1 receptors (AT1Rs) in the brain stem between control rats and ovariectomized rats, because estrogen functions upstream of the renin–angiotensin system,[32,33] and the Rho/Rho-kinase pathway is downstream of the renin–angiotensin system.[34,35]

Methods

This study was reviewed and approved by the Committee on the Ethics of Animal Experiments, Kyushu University Graduate School of Medical Sciences, and was conducted according to the Guidelines for Animal Experiments of Kyushu University. Female SHRs (11-week-old, SLC Japan, Hamamatsu, Japan) were used in the present study. A flexible catheter containing an arterial pressure transmitter was introduced into the abdominal aorta just below the renal arteries under sodium pentobarbital (50 mg/kg IP) anesthesia. After surgery, rats were housed singly in cages and allowed unrestricted movement. Rats were fed food devoid of phytoestrogens (AIN 76A, Kyudo Co, Ltd). For 21 days after ovariectomy, arterial pressure and HR were recorded continuously for 10 minutes every other day using a UA-10 telemetry system (Data Sciences International).[25,31]

Surgical Procedures

Seven days after catheter implantation, we performed bilateral ovariectomy (OVX) or sham operation (control) in the then 12-week-old rats under sodium pentobarbital (50 mg/kg IP) anesthesia. Ovariectomized rats were further randomly divided into 2 groups. The first group received continuous infusion of vehicle (a-CSF, 0.25 μL/h; OVX-VEH rats), and the second group received continuous infusion of Y-27632, a specific Rho-kinase inhibitor (5 mmol/L Y-27632, 0.25 μL/h; OVX-Y rats), intracisternally for 2 weeks via a miniosmotic pump (Alzet model 1002; Durect Corp). The miniosmotic pump, filled with vehicle or Y-27632, was implanted subcutaneously in the back and connected to a polyethylene tube (PE 10). A small hole was then made in the atlantooccipital membrane, which covers the dorsal surface of the medulla, and the tip of the tube was placed intracisternally and fixed in place with tissue adhesive. After surgery, the rats were free to move about their cages. The infusion was calculated to last 14 days.

Power Spectral Analysis

To evaluate sympathetic activity, we performed power spectral analysis on day 11 after OVX or sham operation. HR was recorded from 20-minute ECGs performed in awake rats using the radiotelemetry system. The ECG data were calculated using the Powerlab system and Chart 4 software (AD Instruments), and the power spectra of the R–R interval was calculated using the maximum entropy method with MemCalc software (Suwa Trust Co, Ltd). The frequency bands were adapted for analysis in rats: a very low frequency band (VLF) of 0 to 0.25 Hz, a low frequency band (LF) of 0.25 to 0.8 Hz, and a high frequency band (HF) of 0.8 to 2.4 Hz.[36–38]

Western Blot Analysis

The animals of each group (control rats, OVX-VEH rats, and OVX-Y rats) were killed with an overdose of sodium pentobarbital on day 11 after OVX or sham operation, and whole brain stem tissues were obtained. The animals used in this experiment were different from those in which arterial pressure, HR, and ECG were monitored. The tissues were obtained as the whole brain stem to ensure that the same areas from each animal were used and then homogenized in lysing buffer containing 40 mmol/L HEPES, 1% Triton X-100, 10% glycerol, 1 mmol/L Na_3VO_4, and 1 mmol/L phenylmethylsulfonyl fluoride. The tissue lysate was centrifuged, and the supernatant was collected. The protein concentration was determined using a BCA protein assay kit (Pierce Chemical). A protein aliquot (15 μg) from each sample was separated on a 10% sodium dodecyl sulfate–polyacrylamide gel and subsequently transferred onto polyvinylidene difluoride membranes (Immobilon-P membrane, Millipore). Membranes were incubated with rabbit anti-phosphorylated ERM proteins [ezrin (Thr567), radixin (Thr564), and moesin (Thr558)], which are the target proteins of Rho-kinase (this primary antibody was made by Kaibuchi and colleagues[39–42] and has been characterized and used in many previous reports). Membranes were then incubated with a horseradish peroxidase-conjugated horse anti-rabbit IgG antibody (1:10 000). Immunoreactivity was detected by enhanced chemiluminescence autoradiography (ECL Western blotting detection kit, Amersham Pharmacia Biotechnology), and the film was analyzed using NIH Image (developed at the National Institutes of Health and available on the Internet at http://rsb.info.nih.gov/nih-image/). Western blot analysis for AT1R was performed as described above using rabbit anti-AT1R antibody (1:1000, Santa Cruz Biotechnology).

Measurement of Estradiol Concentration in the Serum and CSF

A separate set of 12-week-old female SHRs was divided into 2 groups. In the first group, bilateral OVX alone was performed (OVX rats). In the second group, sham operation was performed (Sham rats). The animals in each group were anesthetized with an overdose of sodium pentobarbital on day 11 after the intervention, and blood samples from the femoral vein were obtained to measure the serum 17β-estradiol concentration by radioimmunoassay performed by SRL Inc). Furthermore, a small hole was made in the atlantooccipital membrane, the tip of a tube connected to a syringe was placed intracisternally, and CSF was collected. Because only a small amount of CSF could be collected from each animal, samples from 5 animals of each group were pooled, and the 17β-estradiol concentration was measured.

Statistical Analysis

All of the values are expressed as mean±SEM. Two-way ANOVA was used to compare differences in mean arterial pressure (MAP) and HR between the Y-27632 and vehicle infusion groups. Comparisons between any mean values were performed by application of Bonferroni's correction for multiple comparisons. An unpaired t test was used to compare the baseline values and the effects of each intervention between groups. Differences were considered to be statistically significant when $P<0.05$.

Results

Effects of OVX and Intracisternal Infusion of Y-27632 on Arterial Pressure and HR Measured by Radiotelemetry

The time course of MAP and HR after OVX and intracisternal infusion of Y-27632 is shown in Figure 1. The baseline

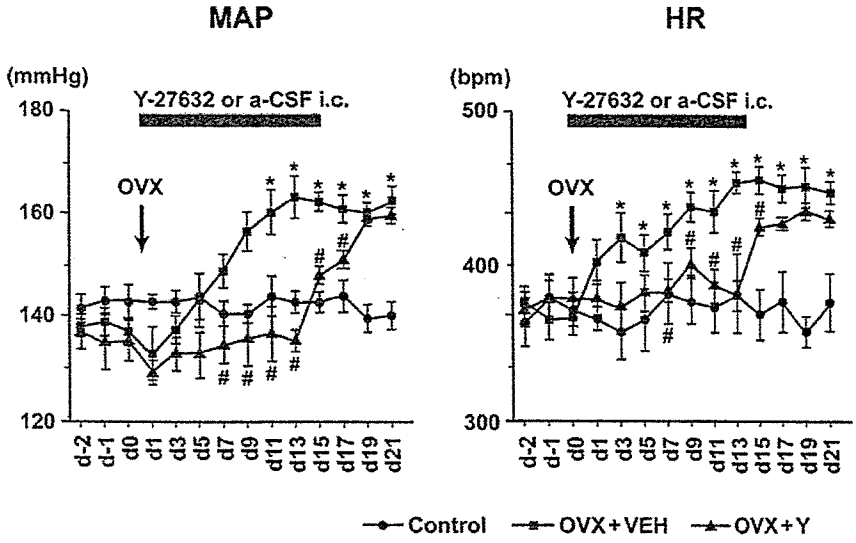

Figure 1. Chronic intracisternal infusion of Y-27632. Time course of MAP and HR after ovariectomy with continuous infusion of Y-27632 or vehicle intracisternally for 2 weeks with a miniosmotic pump. MAP and HR were increased in OVX-VEH rats. Y-27632 significantly attenuated the increase in MAP and HR in OVX-Y rats (n=4 for each). *P<0.05 vs control rats. #P<0.05 vs OVX+VEH rats.

values of arterial pressure in control rats, OVX-VEH rats, and OVX-Y rats were 192±7, 189±9, and 187±7 mm Hg (systolic arterial pressure); 115±3, 113±2, and 112±4 mm Hg (diastolic arterial pressure); and 142±3, 138±2, and 137±3 mm Hg (MAP), respectively. The baseline values of HR in control rats, OVX-VEH rats, and OVX-Y rats were 373±7, 372±6, and 362±7 bpm, respectively. Arterial pressure and HR were significantly increased in OVX-VEH rats. Y-27632 significantly attenuated the increase in arterial pressure and HR in OVX-Y rats. After discontinuing treatment with Y-27632, arterial pressure and HR increased to levels similar to those in OVX-VEH rats. In control rats, arterial pressure and HR did not change after the operation.

Effects of OVX and Intracisternal Infusion of Y-27632 on HR Power Spectra

The effects of OVX on HR power spectra are shown in Figure 2. The VLF and LF components were significantly increased in OVX-VEH rats. The VLF and LF components in OVX-Y rats were significantly reduced compared with those in OVX-VEH rats. The HF component, however, did not differ between control rats, OVX-VEH rats, and OVX-Y rats; therefore, the LF/HF ratio, which is considered to be a measure of sympathovagal balance, was also increased in OVX-VEH rats compared with the other groups.

Western Blot Analysis of Rho-Kinase Activity

The extent of ERM phosphorylation, which represents Rho-kinase activity, was greater in OVX-VEH rats and in OVX-Y rats than in control rats (Figure 3A). The increase in ERM phosphorylation in OVX-Y rats, however, was significantly less than that in OVX-VEH rats. The expression level of the total ERM family did not differ between groups.

AT1R Expression Level

The AT1R expression level was significantly increased in OVX-VEH rats and OVX-Y rats compared with control rats (Figure 3B). The increase in AT1R expression in OVX-Y rats was significantly smaller than that in OVX-VEH rats (Figure 3B).

Effects of OVX on Serum and CSF Estradiol Concentrations

On day 11 after the intervention, the serum 17β-estradiol concentration was decreased in OVX rats compared with Sham rats (139±51 pg/mL versus 34±11 pg/mL; n=5 for each; P<0.05). In addition, the CSF 17β-estradiol concentration was also decreased in OVX rats (270.0 pg/mL versus 61.5 pg/mL).

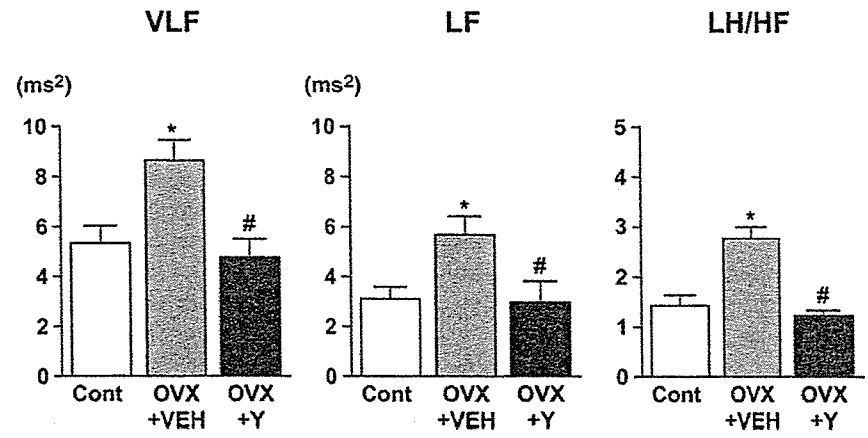

Figure 2. Evaluation of sympathetic nerve activity by power spectral analysis. Each graph shows the power density of each spectrum. The power density of VLF and LF reflects sympathetic nerve activity, and the ratio of LF/HF reflects the sympathovagal balance. Both parameters increased in OVX+VEH rats compared with control rats (n=5 for each). *P<0.05 vs control rats. #P<0.05 vs OVX+VEH rats.

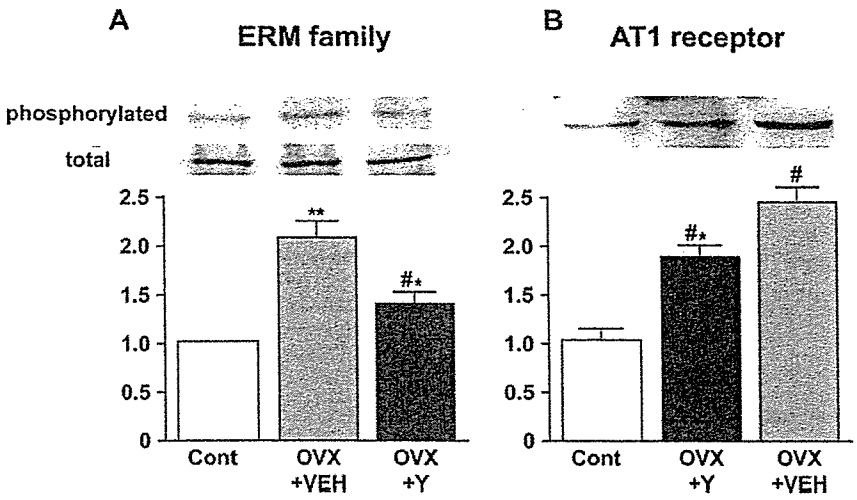

Figure 3. A, Western blot analysis demonstrating p-ERM expression in the brain stem. The p-ERM expression level was significantly higher in OVX-VEH rats than in control rats, and its increase was significantly attenuated by Y-27632 infusion. The data are expressed as the relative ratio to controls. The ratio of phosphorylated/total ERM family expression in control rats was assigned a value of 1 (n=5 for each). $^{**}P<0.01$, $^{*}P<0.05$ vs control rats. $\#P<0.05$ vs OVX+VEH rats. B, Western blot analysis demonstrating AT1R expression in the brain stem. The AT1R expression level was significantly higher in OVX-VEH rats than in control rats, and its increase was significantly attenuated by Y-27632 infusion. The data are expressed as relative ratio to control. The extent of the AT1R in control rats was assigned a value of 1 (n=4 for each). $^{**}P<0.01$, $^{*}P<0.05$ vs control rats. $\#P<0.05$ vs OVX+VEH rats.

Discussion

The present study demonstrated that in female SHRs, OVX induced an increase in arterial pressure via activation of the sympathetic nervous system, attributable, at least in part, to Rho-kinase activation in the brain stem. Furthermore, the results of the present study suggest that angiotensin II in the brain stem contributes to these mechanisms.

We used only female SHRs as a hypertensive model in this study. Previous studies focusing on the interaction between cardiovascular regulation and estrogen demonstrated that OVX has no effect on arterial pressure in normotensive animals.[43,44] Although the Rho-kinase activity and renin–angiotensin system in the brain stem might be affected by OVX in normotensive rats, the effects of OVX, like in postmenopausal women, are more obvious in hypertensive rats than in normotensive rats. Therefore, we used only SHRs in the present study. Previous studies also indicated that OVX alters arterial pressure only in salt-sensitive hypertensive models, such as SHRs and Dahl salt-sensitive rats.[45–47] There are reports that bilateral OVX in hypertensive rats enhances salt sensitivity but only increases arterial pressure in rats fed a high NaCl diet.[45,46] In the present study, arterial pressure and HR were significantly increased in OVX-VEH rats fed a standard NaCl diet compared with controls from day 7 after bilateral OVX. The discrepant results might be because of differences in age at the time of OVX or in the diet. In fact, rats ovariectomized at a young age and fed a normal diet only have a significant increase in arterial pressure when fed a high-NaCl diet,[45,46] whereas rats ovariectomized at an adult age and fed a phytoestrogen-devoid diet have increased arterial pressure under both a standard NaCl diet and a high-NaCl diet.[47] Furthermore, we measured arterial pressure by radiotelemetry. This system allowed us to measure arterial pressure in awake rats under relatively stress-free conditions compared with other methods, such as the tail-cuff method. In a preliminary study, when we measured arterial pressure by the tail-cuff method, OVX tended to increase arterial pressure, but the difference was not significant (data not shown). These methodologic differences might also cause discrepant results from previous studies. In fact, arterial pressure measured by radiotelemetry is significantly increased in ovariectomized Dahl salt-sensitive rats fed a phytoestrogen-free and low-salt diet.[48]

Intracisternal infusion of Y-27632 prevented the OVX-induced increase in arterial pressure, suggesting that endogenous Rho-kinase in the brain stem has an important role in OVX-induced hypertension in female SHRs. The concentration of Y-27632 (5 mmol/L) used in the present study has selective effects on the CNS.[26] Intracisternal drug infusion affects neurons in several regions of the autonomic cardiovascular area. We demonstrated previously, however, that the Rho/Rho-kinase pathway is activated in the NTS of SHRs but not normotensive rats, and Rho-kinase inhibition in the NTS induces a significant reduction in arterial pressure.[25] In addition, the NTS is positioned at the dorsal surface of the medulla. Therefore, Y-27632 might have greater effects on neurons of the NTS than on neurons of other nuclei, although we cannot exclude the possibility that it affects other autonomic areas in the brain stem. Together, these findings suggest that the effect of Y-27632 is mediated in part by the inhibition of Rho-kinase activity in the NTS.

In the present study, it is unlikely that the results are because of nonspecific effects caused by the surgical procedure, because continuous intracisternal infusion of vehicle using the same device did not suppress the increase in arterial pressure, and after discontinuing the Y-27632 infusion, arterial pressure increased to levels similar to those in OVX-VEH rats. In addition, ERM phosphorylation in the brain stem was significantly increased in OVX-VEH rats and reduced in OVX-Y rats, which strongly suggests that the Rho-kinase activity in the brain stem of OVX-VEH rats was increased and that Y-27632 suppressed Rho-kinase activity. We estimated the extent of ERM phosphorylation as a marker of Rho-kinase activity. The ERM family members are concentrated in the actin-rich cell surface, cross-link actin filaments with the plasma membrane, and contribute to cell–cell adhesion and maintenance of cell shape and cell motility.[49] Although the role of ERM family members in the central cardiovascular regulation is not clear, and ERM family members might be the substrates of other kinases, ERM phosphorylation is commonly used as an indicator of Rho-kinase activity.[25,26,34,40–42]

In the present study, intracisternal infusion of Y-27632 nearly abolished the OVX-induced increase in arterial pressure. We reported previously that Rho-kinase activity in the brain stem of hypertensive rats is increased compared with normotensive rats.[25,26] Therefore, intracisternal infusion of Y-27632 might suppress not only the OVX-induced increase in Rho-kinase activity but also basal Rho-kinase activity, thereby inducing a greater reduction in arterial pressure than that induced by OVX. In most previous studies, arterial pressure changes were evaluated several weeks after OVX. In the present study, ≈1 week after OVX, arterial pressure of ovariectomized rats was significantly increased compared with that of control rats. As mentioned above, we used more sensitive methods for measuring arterial pressure. In addition, we confirmed that the 17β-estradiol concentration, both in the serum and the CSF, decreased by ≈25% at 11 days after OVX. Although the serum and the CSF estradiol concentrations were markedly decreased by OVX, the concentrations were still high. We speculate that other organs, such as adrenal glands or adipocytes, produced estradiol after OVX. We did not address these issues, however, and do not have precise interpretations for this finding. In the present study, we primarily wanted to confirm that OVX reduced serum and CSF estradiol concentrations.

We estimated sympathetic activity using the HRV power spectral analysis. HRV is used as a noninvasive marker of autonomic outflow to the heart in a variety of disease states.[50] HRV has a very specific pattern in the frequency domains delineated by the HF, LF, and VLF components.[36] Spontaneous VLF power, which is 0 to 0.25 Hz, and LF power, which is 0.25 to 0.8 Hz, in the rat are particularly related to sympathetic nerve activity.[36–38] In fact, an increased LF component in R–R variability occurs in various conditions known to decrease baroreflex gain and increase sympathetic outflow, such as tilt, mental stress, and exercise.[51] On the other hand, the HF component is attributed to vagal and respiratory control, and the LF/HF ratio is used as an index of sympathovagal balance.[52] Therefore, we also used spectral analysis of the HR in the present study. The VLF and LF powers or the LF/HF ratio were greater in OVX-VEH rats than in control rats, and those in OVX-Y rats were significantly reduced compared with OVX-VEH rats. Furthermore, the HR increase could also be an indicator of activation of the sympathetic nervous system. In the present study, HR was greater in OVX-VEH rats than in control rats and that in OVX-Y rats was significantly reduced compared with OVX-VEH rats. These results indicate that sympathetic activity was increased by OVX, and intracisternal infusion of Y-27632 significantly attenuated the increase in sympathetic activity.

Estrogen decreases arterial pressure by acting on blood vessels or the kidney via the AT1R.[5,6,41] Furthermore, the renin–angiotensin system is also a major pathway of the central mechanisms of hypertension. Previous reports suggest that angiotensin II contributes to the neural mechanisms of hypertension.[53,54] In addition, inhibition of Rho-kinase activity suppresses angiotensin II–induced cardiovascular effects.[34] Therefore, we examined AT1R expression levels in each group to address the possibility of a partial interaction between the renin–angiotensin system and the Rho/Rho-kinase pathway in OVX-induced hypertension. The AT1R levels in the brain stem were significantly increased by OVX, and this increase was attenuated by intracisternal infusion of Y-27632. These results suggested that angiotensin II in the brain stem contributes to the mechanisms of OVX-induced hypertension in female SHRs. The Rho/Rho-kinase pathway is downstream of the renin–angiotensin system.[34,35] RhoA regulates the expression of AT1R,[55] however, and Y-27632 inhibits not only Rho-kinase activity, but also RhoA activity.[56] Therefore, Y-27632 might attenuate RhoA activity by direct effects or negative feedback mechanisms of the Rho/Rho-kinase pathway and, thus, lead to the inhibition of AT1R expression. The finding that Y-27632 had only a weak effect on AT1R expression, together with the results of previous studies,[34,35] suggest that the depletion of endogenous estrogen activates the Rho/Rho-kinase pathway in the brain stem and might also activate the renin–angiotensin system.

In conclusion, we demonstrated that the depletion of endogenous estrogen by OVX increases arterial pressure in female SHRs, at least in part, via activation of the renin–angiotensin system and Rho/Rho-kinase pathway in the brain stem.

Perspectives

It is not known how OVX induces increases in arterial pressure in female SHRs. In the CNS, both the Rho/Rho-kinase pathway and estrogen regulate the formation of excitatory synapses on dendritic spines.[27] Dendritic spines form the postsynaptic contact sites of excitatory synapses in the CNS[22] and are associated with glutamate sensitivity.[23] Therefore, estrogen depletion might induce morphological or functional changes in the dendritic spines via Rho-kinase activation. On the other hand, estrogen depletion increases arterial pressure and hypothalamic norepinephrine levels,[46] and hypothalamus neurons project to the dorsomedial medulla neurons, such as those in the NTS.[57] These findings suggest that estrogen depletion affects dorsomedial medulla neurons via changes in the hypothalamic norepinephrine levels. Although further studies are needed to clarify the mechanisms of these effects, the Rho/Rho-kinase pathway in the brain stem might be involved in the mechanisms underlying OVX-induced hypertension, because Rho-kinase in the NTS is involved in central mechanisms of cardiovascular regulation via modulation of the sensitivity of NTS neurons to glutamate.[24–26,58]

Sources of Funding

This study was supported by Grants-in-Aid for Scientific Research from the Japan Society for the Promotion of Science (S18659230, A15200040, C17590745), and by a Grant for Research on the Autonomic Nervous System and Hypertension from Kimura Memorial Heart Foundation/Pfizer Pharmaceuticals, Inc.

Disclosures

None.

References

1. Hayes SN, Taler SJ. Hypertension in women: current understanding of gender difference. *Mayo Clin Proc.* 1998;73:157–165.
2. Khoury S, Yarrows SA, O'Brien TK, Sowers J. Ambulatory blood pressure monitoring in nonacademic setting: effects of age and sex. *Am J Hypertens.* 1992;5:616–623.

3. Wiinber N, Hoegholm A, Benzton MWE. 24-Hr ambulatory blood pressure in 352 normal Danish subjects related to age and gender. *Am J Hypertens.* 1995;8:978–986.
4. Kannel WB, Wilson PW. Risk factors that attenuate the female coronary disease advantage. *Arch Intern Med.* 1995;155:57–61.
5. Dubey RK, Oparil S, Imthurm B, Jackson EK. Sex hormones and hypertension. *Cardiovasc Res.* 2002;53:688–708.
6. Mendelsohn ME, Karas RH. The protective effects of estrogen on the cardiovascular system. *N Engl J Med.* 1999;340:1801–1811.
7. Pamidimukkala J, Taylor JA, Welshons WV, Lubahn DB, Hay M. Estrogen modulation of baroreflex function in conscious mice. *Am J Physiol.* 2003;284:R983–R989.
8. Huikuri HV, Pikkujamsa SM, Airaksinen J, Ikaheimo MJ, Rantala AO, Kauma H, Lilja M, Kesaniemi A. Sex-related differences in autonomic modulation of heart rate in middle–aged subjects. *Circulation.* 1996;94: 122–125.
9. Vongpatanasin W, Tuncel M, Mansour Y, Arbique D, Victor RG. Transdermal estrogen replacement therapy decreases sympathetic activity in postmenopausal women. *Circulation.* 2001;103:2903–2908.
10. McEwen BS, Alves SE. Estrogen action in the central nervous system. *Endocr Rev.* 1999;20:279–307.
11. Blaustein JD, Lehman MN, Turcotte JC, Greene G. Estrogen receptors in dendrites and axon terminals in guinea pig hypothalamus. *Endocrinology.* 1992;131:281–290.
12. Haywood SA, Simonian SX, van der Beek EM, Bicknell RJ, Herrison AE. Fluctuating estrogen and progesterone receptor expression in brainstem norepinephrine neurons through the rat estrous cycle. *Endocrinology.* 1999;140:3255–3263.
13. Saleh MC, Connell BJ, Saleh TM. Autonomic and cardiovascular reflex responses to central estrogen injection in ovariectomized female rats. *Brain Res.* 2000;879:105–114.
14. Saleh MC, Connell BJ, Saleh TM. Medullary and intrathecal injections of 17β-estradiol in male rats. *Brain Res.* 2000;867:200–209.
15. Kimura K, Ito M, Amano M, Chihara K, Fukata Y, Nakafuku M, Yamamori B, Feng J, Nakano T, Okawa K, Iwamatsu A, Kaibuchi K. Regulation of myosin phosphatase by Rho and Rho-associated kinase (Rho-kinase). *Science.* 1996;273:245–248.
16. Kawano Y, Fukata Y, Oshiro N, Amano M, Nakamura T, Ito M, Matsumura F, Inagaki M, Kaibuchi K. Phosphorylation of myosin binding subunit(MBS) of myosin phosphatase by Rho-kinase in vivo. *J Cell Biol.* 1999;147:1023–1037.
17. Shimokawa H. Rho-kinase as a novel therapeutic target in treatment of cardiovascular disease. *J Cardiovasc Pharmacol.* 2002;39:319–327.
18. Loirand G, Guérin P, Pacaud P. Rho kinase in cardiovascular physiology and pathophysiology. *Circ Res.* 2006;98:322–334.
19. Mukai Y, Shimokawa H, Matoba T, Kandabashi T, Satoh S, Hiroki J, Kaibuchi K, Takeshita A. Involvement of Rho-kinase in hypertensive vascular disease: a novel therapeutic target in hypertension. *FASEB J.* 2001;15:1062–1064.
20. Masumoto A, Hirooka Y, Shimokawa H, Hironaga K, Setoguchi S, Takeshita A. Possible involvement of Rho-kinase in the pathogenesis of hypertension in humans. *Hypertension.* 2001;38:1307–1310.
21. Nakayama AY, Harms MB, Luo L. Small GTPases Rac and Rho in the maintenance of dendritic spines and branches in hippocampal pyramidal neurons. *J Neurosci.* 2000;20:5329–5338.
22. Koch C, Zador A. The function of dendritic spines: devices subserving biochemical rather than electrical compartmentalization. *J Neurosci.* 1993;13:413–422.
23. Matsuzaki M, Ellis-Davies GC, Nemoto T, Miyashita Y, Iino M, Kasai H. Dendritic spine geometry is critical for AMPA receptor expression in hippocampal CA1 pyramidal neurons. *Nat Neurosci.* 2001;4:1086–1092.
24. Ito K, Hirooka Y, Hori N, Kimura Y, Sagara Y, Shimokawa H, Takeshita A, Sunagawa K. Inhibition of Rho-kinase in the nucleus tractus solitarius enhances glutamate sensitivity in rats. *Hypertension.* 2005;46:360–365.
25. Ito K, Hirooka Y, Sakai K, Kishi T, Kaibuchi K, Shimokawa H, Takeshita A. Rho/Rho-kinase pathway in brain stem contributes to blood pressure regulation via sympathetic nervous system. *Circ Res.* 2003;92: 1337–1343.
26. Ito K, Hirooka Y, Kishi T, Kimura Y, Kaibuchi K, Shimokawa H, Takeshita A. Rho/Rho-kinase pathway in the brainstem contributes to hypertension caused by chronic nitric oxide synthase inhibition. *Hypertension.* 2004;43:156–162.
27. Mcewen BS, Tanapat P, Weiland NG. Inhibition of dendritic spine induction on hippocampal CA1 pyramidal neurons by a nonsteroidal estrogen antagonist in female rats. *Endocrinology.* 1999;140:1044–1047.
28. Gould E, Woolley C, Frankfurt M, McEwen BS. Gonadal steroids regulate dendritic spine density in hippocampal pyramidal cells in adulthood. *J Neurosci.* 1990;10:1286–1291.
29. Woolley C, McEwen BS. Roles of estradiol and progesterone in regulation of hippocampal dendritic spine density during the estrous cycle in the rat. *J Comp Neurol.* 1993;336:293–306.
30. Uehata M, Ishizaki T, Satoh H, Ono T, Kawahara T, Morishita, Tamakawa H, Yamagami K, Inui J, Maekawa M, Narumiya S. Calcium sensitization of smooth muscle mediated by a Rho-associated protein kinase in hypertension. *Nature.* 1997;389:990–994.
31. Sakai K, Hirooka Y, Matsuo I, Eshima K, Shigematsu H, Shimokawa H, Takeshita A. Overexpression of eNOS in NTS causes hypotension and bradycardia in vivo. *Hypertension.* 2000;36:1023–1028.
32. Gragasin FS, Xu Y, Arenas IA, Kainth N, Davidge ST. Estrogen reduces angiotensin II-induced nitric oxide synthase and NAD(P)H oxidase expression in endothelial cells. *Arterioscler Thromb Vasc Biol.* 2003;23: 38–44.
33. Gallagher PE, Li P, Lenhart JR, Chappell MC, Brosnihan KB. Estrogen regulation of angiotensin-converting enzyme mRNA. *Hypertension.* 1999;33[part II]:323–328.
34. Higashi M, Shimokawa H, Hattori T, Hiroki J, Mukai Y, Morikawa K, Ichiki T, Takahashi S, Takeshita A. Long-term inhibition of Rho-kinase suppresses angiotensin II-induced cardiovascular hypertrophy in rats in vivo. Effect on endothelial NAD(P)H oxidase system. *Circ Res.* 2003; 93:767–775.
35. Funakoshi Y, Ichiki T, Shimokawa H, Egashira K, Takeda K, Kaibuchi K, Takeya M, Yoshimura T, Takeshita A. A critical role of Rho-kinase in angiotensin II-induced monocyte chemoattractant protein-1 expression in rat vascular smooth muscle cells. *Hypertension.* 2001;38:100–104.
36. Kuo TBJ, Yang CCH. Altered frequency characteristic of central vasomotor control in SHR. *Am J Physiol.* 2000;278:H201–H207.
37. Cerutti C, Barres C, Paultre C. Baroreflex modulation of blood pressure and heart rate variabilities in rats: assessment by spectral analysis. *Am J Physiol.* 1994;266:H1993–H2000.
38. Cerutti C, Gustin MP, Paultre M, Julien LC, Vincent JM, Sassard J. Autonomic nervous system and cardiovascular variability in rats: a spectral analysis approach. *Am J Physiol.* 1991;261:H1291–H1299.
39. Matsui T, Maeda M, Doi Y, Yonemura S, Amano M, Kaibuchi K, Tsukita S. Rho-kinase phosphorylates COOH-terminal threonines of Ezrin/ Radixin/Moesin (ERM) proteins and regulates their head-to-tail association. *J Cell Biol.* 1998;140:647–657.
40. Morishige K, Shimokawa H, Eto Y, Kandabashi T, Miyata K, Matsumoto Y, Hoshijima M, Kaibuchi K, Takeshita A. Adenovirus-mediated transfer of dominant-negative Rho-kinase induces a regression of coronary arteriosclerosis in pigs in vivo. *Arterioscler Thromb Vasc Biol.* 2001;21: 548–554.
41. Takemoto M, Sun J, Hiroki J, Shimokawa H, Liao JK. Rho-kinase mediates hypoxia-induced downregulation of endothelial nitric oxide synthase. *Circulation.* 2002;106:57–62.
42. Matsumoto Y, Uwatoku T, Oi K, Abe K, Hattori T, Morishige K, Eto Y, Fukumoto Y, Nakamura K, Shibata Y, Matsuda T, Takeshita A, Shimokawa H. Long-term inhibition of Rho-kinase suppresses neointimal formation after stent implantation in porcine coronary arteries: involvement of multiple mechanisms. *Arterioscler Thromb Vasc Biol.* 2004;24:181–186.
43. Mohamed MK, El-Mas MM, Abdel AA. Estrogen enhancement of baroreflex sensitivity is centrally mediated. *Am J Physiol.* 1999;276: R1030–R1037.
44. Pamidimukkala J, Taylor JA, Welshons WV, Lubahn DB, Hay M. Estrogen modulationof baroreflex function in conscious mice. *Am J Physiol.* 2003;284:R983–R989.
45. Harrison-Bernard LM, Schulman IH, Raij L. Postovariectomy hypertension is linked to increased renal AT1 receptor and salt sensitivity. *Hypertension.* 2003;42:1157–1163.
46. Fang Z, Carlson SH, Chen YF, Oparil S, Wyss JM. Estrogen depletion induces NaCl-sensitive hypertension in female spontaneously hypertensive rats. *Am J Physiol.* 2001;281:R1934–R1939.
47. Peng N, Clark JT, Wei C-C, Wyss JM. Estrogen depletion increases blood pressure and hypothalamic norepinephrine in middle-aged spontaneously hypertensive rats. *Hypertension.* 2003;41:1164–1167.
48. Hinojosa-Laborde C, Craig T, Zheng W, Ji H, Haywood JR, Sandberg K. Ovariectomy augments hypertension in aging female dahl salt-sensitive rats. *Hypertension.* 2004;44:405–409.
49. Louvet-Vallée S. ERM proteins: From cellular architecture to cell signaling. *Biol Cell.* 2000;92:305–316.

50. Task Force of the European Society of Cardiology and the North Am Society of Pacing and Electrophysiology. Heart rate variability. Standards of measurement, physiological interpretation, and clinical use. *Eur Heart J.* 1996;17:354–381.
51. Lanfranchi PA, Somers VK. Arterial baroreflex function and cardiovascular variability: interactions and implications. *Am J Physiol.* 2002;283: R815–R826.
52. Pagani M, Lombardi F, Guzzetti S, Rimoldi O, Furlan R, Pizzinelli P, Sandrone G, Malfatto G, Dell'Orto S, Piccaluga E. Power spectral analysis of heart rate and arterial pressure variabilities as a marker of sympatho-vagal interaction in man and conscious dog. *Circ Res.* 1986; 59:178–193.
53. Matsumura K, Averill DB, Ferrario CM. Angiotensin II acts at AT1 receptors in the nucleus of the solitary tract to attenuate the baroreceptor reflex. *Am J Physiol.* 1998;275:R1611–R1619.
54. Eshima K, Hirooka Y, Shigematsu H, Matsuo I, Koike G, Sakai K, Takeshita A. Angiotensin in the nucleus tractus solitarii contributes to neurogenic hypertension caused by chronic nitric oxide synthase inhibition. *Hypertension.* 2000;36:259–263.
55. Ichiki T, Takeda K, Tokunou T, Iino N, Egashira K, Shimokawa H, Hirano K, Kanaide H, Takeshita A. Downregulation of angiotensin II type 1 receptor by hydrophobic 3-hydroxy-3-methylglutaryl coenzyme A reductase inhibitors in vascular smooth muscle cells. *Arterioscler Thromb Vasc Biol.* 2001;21:1896–1901.
56. Kobayashi N, Nakano S, Mita S, Kobayashi T, Honda T, Tsubokou Y, Matsuoka H. Involvement of Rho-kinase pathway for angiotensin II-induced plasminogen activator inhibitor-1 gene expression and cardiovascular remodeling in hypertensive rats. *J Pharmacol Exp Therap.* 2002;301:459–466.
57. Nishimura H, Oomura Y. Effects of hypothalamic stimulation on activity of dorsomedial medulla neurons that respond to subdiaphragmatic vagal stimulation. *J Neurophysiol.* 1987;58:655–675.
58. Ito K, Hirooka Y, Sagara Y, Kimura Y, Kaibuchi K, Shimokawa H, Takeshita A, Sunagawa K. Inhibition of Rho-kinase in the brainstem augments baroreflex control of heart rate in rats. *Hypertension.* 2004;44:478–483.

ELSEVIER

Cardiovascular Research 72 (2006) 184–190

Cardiovascular Research

www.elsevier.com/locate/cardiores

Telmisartan downregulates angiotensin II type 1 receptor through activation of peroxisome proliferator-activated receptor γ

Ikuyo Imayama, Toshihiro Ichiki *, Keita Inanaga, Hideki Ohtsubo, Kae Fukuyama, Hiroki Ono, Yasuko Hashiguchi, Kenji Sunagawa

Department of Cardiovascular Medicine, Kyushu University Graduate School of Medical Sciences, 3-1-1 Maidashi, Higashi-ku, 812-8582 Fukuoka, Japan

Received 2 May 2006; received in revised form 4 July 2006; accepted 6 July 2006
Available online 21 July 2006
Time for primary review 26 days

Abstract

Objective: Telmisartan, an angiotensin II type 1 receptor (AT1R) antagonist, was found to have a unique property: it is a partial agonist of peroxisome proliferator-activated receptor gamma (PPARγ). Since previous studies have demonstrated that PPARγ activators suppressed AT1R expression, we examined whether telmisartan affects AT1R expression in vascular smooth muscle cells.

Methods: Vascular smooth muscle cells were derived from the thoracic aorta of Wistar–Kyoto rat. Northern and Western blotting analysis were used to examine AT1R mRNA and protein expression, respectively. The DEAE-dextran method was used for transfection, and the promoter activity of AT1R was examined by luciferase assay.

Results: Telmisartan decreased the expression of AT1R at the mRNA and protein levels in a dose- and time-dependent manner. Decreased AT1R promoter activity with unchanged mRNA stability suggested that telmisartan suppressed AT1R gene expression at the transcriptional level. However, the expression of AT1R was not suppressed by other AT1R antagonists such as candesartan or olmesartan. Since the suppression of AT1R expression was prevented by pretreatment with GW9662, a PPARγ antagonist, PPARγ should have participated in the process. The deletion and mutation analysis of the AT1R gene promoter indicated that a GC box located in the proximal promoter region is responsible for the telmisartan-induced downregulation.

Conclusion: Our data provides a novel insight into an effect of telmisartan: telmisartan inhibits AT1R gene expression through PPARγ activation. The dual inhibition of angiotensin II function by telmisartan – AT1R blockade and downregulation – would contribute to more complete inhibition of the renin–angiotensin system.

Keywords: Antihypertensive; Diuretic drugs; Atherosclerosis; Gene expression; Receptors; Renin–angiotensin system

1. Introduction

Angiontensin (Ang) II is a main final effector molecule of the renin–angiotensin system. Physiologically, Ang II plays an important role in controlling the blood pressure and the fluid volume [1]. However, Ang II is also involved in pathological conditions such as renal insufficiency [2], cardiovascular diseases [3] and metabolic disorders [4].

The effect of Ang II are mediated by Ang II receptors and so far two isoforms, type 1 receptor (AT1R) and type 2 receptor (AT2R), have been identified [5]. AT1R mediates most of the traditional effects of Ang II such as vasoconstriction, sodium retention, aldosterone secretion, and cell proliferation [1]. In contrast, AT2R mediates vasodilation and growth inhibition that opposes to the effects of AT1R [6]. However, it was reported that AT2R was hardly detected in blood vessel of adult animal [6].

Ang I converting enzyme inhibitors and AT1R antagonists are clinically used. Many clinical trials have demonstrated that these drugs are beneficial in the treatment of heart failure, renal failure and myocardial infarction. These drugs are also useful in preventing new-onset diabetes mellitus [7] and atrial fibrillation [8]. Telmisartan (Tel), one of the clinically

* Corresponding author. Tel.: +81 92 642 5361; fax: +81 92 642 5374.
E-mail address: ichiki@cardiol.med.kyushu-u.ac.jp (T. Ichiki).

0008-6363/$ - see front matter © 2006 European Society of Cardiology. Published by Elsevier B.V. All rights reserved.
doi:10.1016/j.cardiores.2006.07.014

available AT1R antagonists, was recently reported to have a partial agonistic effect on peroxisome proliferator activated receptor gamma (PPARγ) [9,10]. PPARγ is a nuclear receptor that regulates specific gene transcription [11]. The target genes of PPARγ are involved in the regulation of lipid and glucose metabolism [12], and inflammatory responses. Moreover, several studies have demonstrated that PPARγ activators are effective in preventing atherogenesis [13,14]. Therefore, Tel is focused for its additional therapeutic values in patients with metabolic disorders.

Previously, we and another group reported that activators of PPARγ such as 15-deoxy-$\Delta^{12,14}$-prostaglandin J_2 and pioglitazone (Pio) decreased the expression of AT1R in vascular smooth muscle cells (VSMCs) [15,16]. We, therefore, examined whether Tel, a partial agonist of PPARγ, affects the expression of AT1R in a similar way to PPARγ agonists in VSMCs.

2. Materials and methods

2.1. Materials

Tel and olmesartan (Olm) were generous gifts from Boehringer Ingelheim Co. and Sankyo Co., respectively. Candesartan (Can) and Pio were provided by Takeda Pharmaceutical Company. Dulbecco's modified Eagle's medium (DMEM) and fetal bovine serum (FBS) were purchased from GIBCO BRL. Bovine serum albumin (BSA) and Actinomycin D (ActD) were purchased from Sigma Chemical Co. Rabbit polyclonal antibody against AT1R [17,18] and α-tubulin were from Santa Cruz Biotechnology. Mouse polyclonal antibody against pERK and rabbit polyclonal antibody against ERK were from Cell Signaling Technology, Inc. Horseradish peroxidase-conjugated secondary antibodies (anti-rabbit IgG and anti-mouse IgG) were purchased from VECTOR Laboratories Inc. [α-^{32}P] dCTP was purchased from Perkin-Elmer Life Sciences.

2.2. Cell culture

All procedures and care of the animals were approved by the Committee on Ethics of Animal Experiments, Kyushu University and this study conforms with the Guide for the Care and Use of Laboratory Animals published by the US National Institutes of Health (NIH Publication No. 85-23, revised 1996). VSMCs were isolated from the thoracic aorta of Wistar–Kyoto rat by an explant method and maintained in DMEM supplemented with 10% FBS at 37 °C in a humidified atmosphere of 95% air −5% CO_2. VSMCs were cultured until grown to confluence, cultured in DMEM with 0.1% BSA for additional 2 days and used in the experiment. Cells between passages 4 and 14 were used.

2.3. Northern blotting

Total RNA was prepared by acid guanidinium thiocyanate–phenol–chloroform extraction method [19]. Total RNA was electrophoresed on a 1.0% agarose, 1.0% formaldehyde gel, transferred to Hybond-N+ membrane (Amersham Biosciences) by a capillary transfer method in 10×SSC (1×SSC is 150 mmol/L of sodium and 15 mmol/L of sodium citrate) buffer overnight. The membrane was cross-linked by a UV cross-linker (Funakoshi Corporation). Prehybridization and hybridization were performed in a buffer containing 50% formamide, 5×SSC, 80 mmol/L sodium phosphate (pH 7.5), 2×Denhardt's Solution, 1% SDS, and 100 μg/L of heat-denatured salmon sperm DNA for 1 h and 16 h, respectively, at 42 °C. An ECORI fragment of the third exon of rat AT1A gene [20] and ribosomal RNA were labeled with ^{32}P by a Random Primer DNA Labeling Kit Ver.2 (Takara Bio Inc.) and used as a probe after heat denaturation. The hybridized membrane was washed twice with 2×SSC at room temperature, followed by two washes with 2×SSC/1% SDS for 30 min at 55 °C. The membrane was then exposed to a KODAK BioMax XAR Film at −80 °C. The hybridized membrane was stripped by boiling in 0.5% SDS solution and hybridized to a ^{32}P-labeled ribosomal RNA probe to obtain reference for the amount of applied RNA. Autoradiography was scanned and analyzed by a MacBAS Bioimage Analyzer (Fuji Photo Film Co). To analyze mRNA stability of AT1R, Actinomycin (Act) D (5 μg/mL) was added after 6 h of stimulation with Tel (10 μmol/L). In a control experiment, only ActD was added. Cells were harvested after 3, 6, 12, and 24 h of addition of ActD and expression level of AT1R mRNA was examined by Northern blot analysis.

2.4. Measurement of AT1R gene promoter activity

Five deletion mutants of AT_{1A} gene promoter were prepared by digestion with restriction endonucleases and

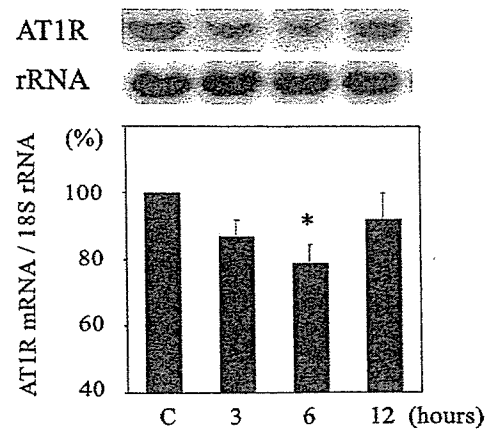

Fig. 1. Telmisartan (Tel) suppressed AT1R mRNA expression in VSMCs. VSMCs were incubated with Tel (10 μmol/L) for various periods as indicated in the figure. Total RNA was isolated and expression of AT1R mRNA and 18S rRNA (rRNA) was determined by Northern blot analysis. Radioactivity of AT1R mRNA was measured with an imaging analyzer and was normalized by radioactivity of rRNA. Values (mean±S.E.M.) are expressed as a percent of control culture in the bar graph (100%) (n=5). *P<0.05 vs control (c).

ligated to luciferase gene [21]. Confluent VSMCs were split by trypsin/EDTA solution and cells were prepared in a 6 cm tissue culture dish. At 80% confluence, 5 μg of AT1 promoter-luciferase fusion DNA and 2 μg of β-galactosidase gene were introduced to VSMC by the DEAE-dextran method according to the manufacturer's instruction (Promega Corporation). The cells were cultured in DMEM with 10% FBS for 18 h, washed twice with phosphate buffered saline, cultured in DMEM with 0.1% BSA for 24 h and stimulated with Tel (10 μmol/L) for 12 h. Then, the cells were lysed in 200 μL of Reporter lysis buffer (Promega Corporation). 100 μL of lysate was used for luciferase activity assay in a Lumat luminometer (LB 9501, Berthold, Germany). The β-galactosidase activity in the same sample was measured spectrophotometrically according to Sambrook et al. [22] and used to normalize the luciferase activity.

The AT1R promoter-luciferase construct with mutation in the GC-box-related sequence (wild type: TGCAGAGCAGC GACGCCCCCTAGGC mutant: TGCAGAGCAGCGA CGTTTCCTAGGC) was a generous gift from Dr. Sugawara (Tohoku University) [16].

2.5. Western blot analysis

VSMCs were lysed in a lysis buffer containing RIPA (100 mM sodium, 60 mM Na_2HPO_4, 100 mM NaF 10 mM EDTA, and 20 mM Tris), 1% aprotinin, 0.5% pepstatin A, 1 mmol/L PMSF, and 0.05% leupeptin. Protein concentrations were determined with the bicinchoninic acid protein assay kit (Pierce Chemical Co). Cell lysates were heated in a sample buffer (62.5 mmol/L Tris–HCl [pH 6.8], 10% glycerol, 2% SDS, 0.05% bromophenolblue, and

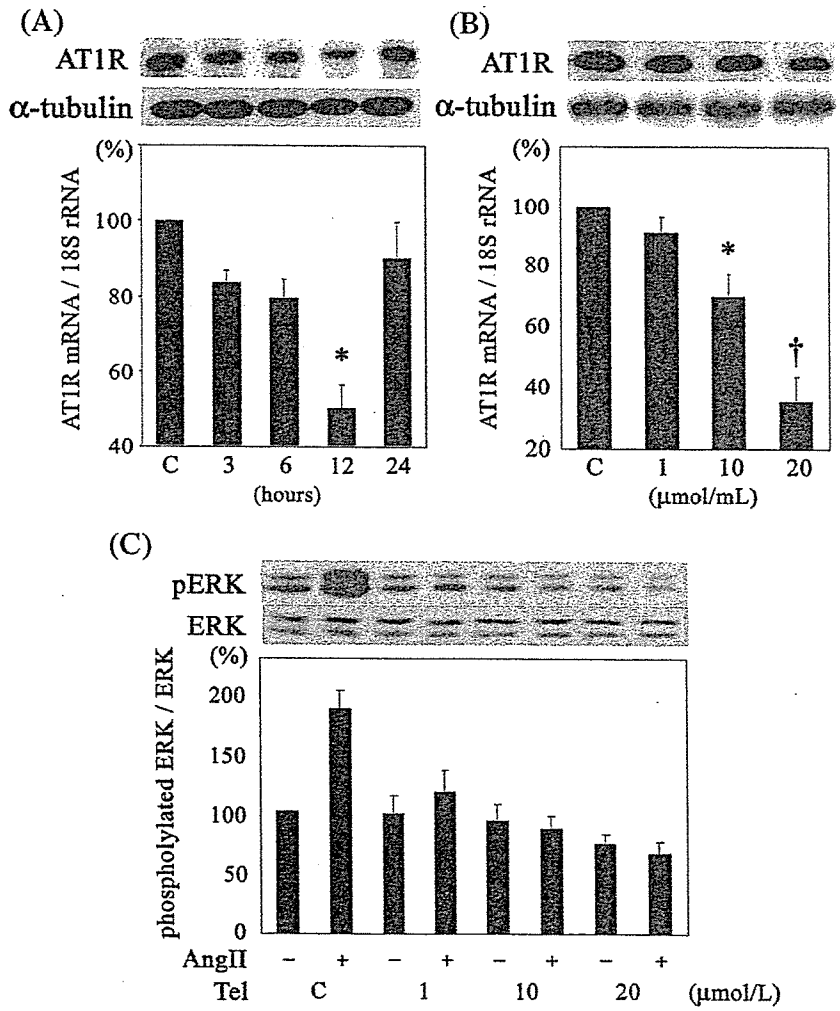

Fig. 2. Suppression of AT1R protein by telmisartan (Tel) in VSMCs. (A) VSMCs were incubated with Tel (10 μmol/L) for various periods as indicated in the figure. (B) VSMCs were incubated with Tel at concentrations varying from 1 to 20 μmol/L for 12 h. Expression of AT1R protein and α-tubulin was detected by Western blot analysis. The density of the specific band was scanned and quantified with an imaging analyzer. The ratio of AT1R to α-tubulin is shown in the bar graph. (C) VSMCs were incubated with Tel at various concentrations as indicated in the figure and stimulated by Ang II (100 μmol/L). Expressions of pERK and ERK protein were detected by Western blot analysis. The density of the specific band was scanned and quantified with an imaging analyzer. The ratio of pERK to ERK is shown in the bar graph. Values (mean±S.E.M.) are expressed as a percent of control (c) culture (100%) ($n=5$). *$P<0.05$ vs control. †$P<0.01$ vs control.

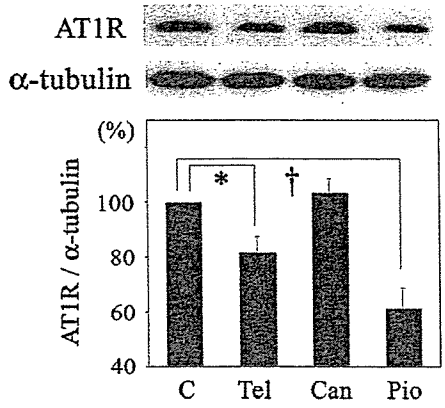

Fig. 3. Suppression of AT1R protein by telmisartan (Tel) but not by candesartan (Can) in VSMCs. VSMCs were incubated with Tel (10 μmol/L, 12 h), Can (10 μmol/L, 12 h), and Pio (10 μmol/L, 6 h). Expression of AT1R protein and α-tubulin was determined by Western blot analysis. Densitometric analysis was performed as described in the legend to Fig. 2. Values (mean±S.E.M.) are expressed as a percent of control (c) culture (100%) (n=5). *P<0.05 vs control. †P<0.01 vs control.

715 mmol/L 2-mercaptoethanol) at 95 °C for 3 min, electrophoresed on 12% SDS-polyacrylamide gel, and transferred to a polyvinylidene difluoride membrane (Immobilon-P, Millipore). The blots were blocked with TBS-T (20 mmol/L Tris–HCl [pH 7.6], 137 mmol/L NaCl, 0.1% Tween 20) containing 5% skim milk at room temperature for 30 min. The AT1R protein expressions were detected by ECL chemiluminescence (Amersham Pharmacia Biotech) according to the manufacturer's instructions. The membranes were exposed to X-ray film. The membranes were stripped by incubating them in a buffer containing 62.5 mmol/L Tris–HCl, 2% SDS, and 100 mmol/L 2-mercaptoethanol at 50 °C for 30 min and reprobed with an antibody against α-tubulin by the same procedure. Phospholylated ERK and ERK (which recognizes both phosphorylated and nonphosphorylated forms) were examined by the same method.

2.6. Statistical analysis

Statistical analysis was performed with 1- or 2-way ANOVA and Fisher test, if appropriate. Statistical significance was designated as P<0.05. Values are expressed as mean±S.E.M.

3. Results

3.1. Tel reduced the expression of AT1R

VMSCs were incubated with Tel (10 μmol/L) for various periods. The expression level of AT1R mRNA was gradually decreased with a peak suppression at 6 h of incubation (Fig. 1). Though we did not remove Tel from the medium, the expression of AT1R demonstrated a transient suppression. The mechanism of its recovery at 12 h of incubation is unknown. However, there are some reports that demonstrated a transient or a biphasic gene expression induced by thiazolidinediones (TZDs) [23,24], which seems to be consistent with our results. Western blot analysis revealed that Tel reduced AT1R protein level with a peak reduction at 12 h of incubation (Fig. 2A), and that Tel suppressed AT1R expression in a dose-dependent manner (Fig. 2B). As shown in Fig. 2C, preincubation with Tel at the same concentration as used in Fig. 2B almost completely inhibited the Ang II-induced ERK phosphorylation.

Following experiment used 10 μmol/L of Tel, which is the minimal dose that suppressed AT1R expression. Pio, one

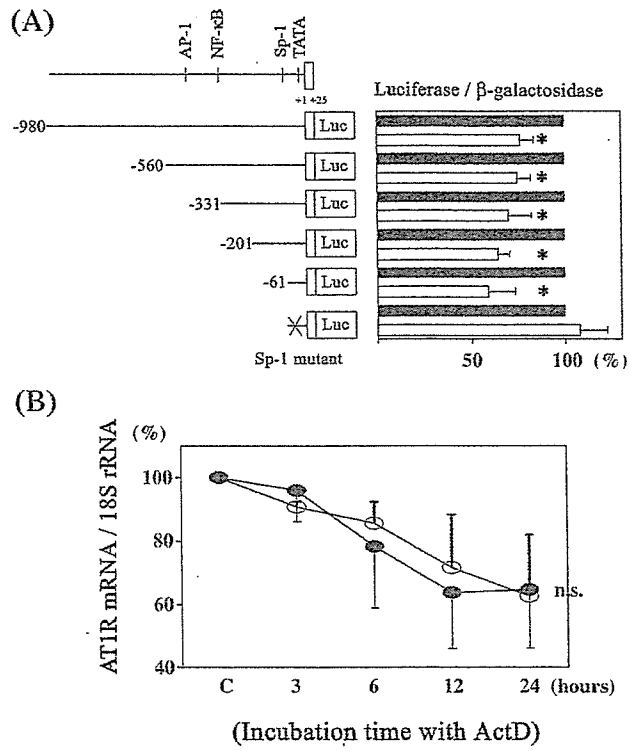

Fig. 4. Effect of telmisartan (Tel) on AT1R gene promoter activity and AT1R mRNA stability. (A) The scheme of deletion mutants of AT1R promoter/luciferase fusion DNA construct and SP-1 mutant construct is indicated. These luciferase constructs were introduced to VSMCs with LacZ expression plasmid by the DEAE-dextran method. Then VSMCs were stimulated with Tel (10 μmol/L) for 12 h. Relative luciferase activity of unstimulated VSMCs (control) was set as 100%. Solid and open bars indicate the relative luciferase activity of unstimulated and Tel-stimulated VSMCs transfected with the same construct indicated in the left panel, respectively. Values (mean±S.E.M.) are expressed as a percent of control culture (n=6). *P<0.05 vs unstimulated cells. n.s. not siginificant. (B) VSMCs were incubated with Tel (10 μmol/L) for 6 h and then ActD (5 μg/mL) was added. In a control experiment, only ActD was added to the medium. Total RNA was isolated at the indicated time after ActD supplementation and expression levels of AT1R mRNA and rRNA were determined with method described in the legend to Fig. 1. Expression level of AT1R mRNA was normalized with that of rRNA. The normalized AT1R mRNA expression before addition of ActD in each group was set as 100% (c), (n=3). n.s. not siginificant.

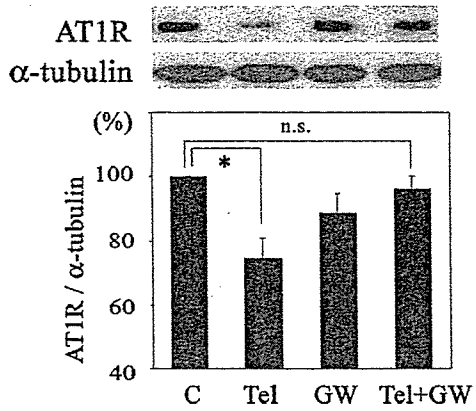

Fig. 5. The effect of GW9662, a PPAR γ antagonist, on telmisartan (Tel)-induced AT1R downregulation. VSMCs were preincubated with GW9662 (5 μg/mL) for 30 min and incubated with or without Tel (10 μmol/L) for 12 h. Expression of AT1R protein and α-tubulin was determined by Western blot analysis. Densitometric analysis was performed as described in the legend to Fig. 2. Values (mean±S.E.M.) are expressed as a percent of control culture (100%) ($n=5$). *$P<0.05$ vs control. n.s. not significant.

of TZDs and a full PPARγ agonist, inhibited AT1R expression as previously described [16]. We examined the effect of other AT1R antagonists on AT1R expression. Can (Fig. 3) and Olm (data not shown) had no effect on AT1R expression.

3.2. Tel inhibits AT1R expression at the transcriptional level

Deletion mutants of AT1 promoter/luciferase fusion DNA were used to locate the response element responsible for Tel-induced AT1R suppression (Fig. 4A). The suppression was observed in all constructs from −980/+25-luc to −61/+25-luc, so we supposed that the response element may exist in the DNA segment between −61 bp and +25 bp. Since Sugawara et al. [16] had previously reported the crucial role of a GC-box-related sequence within the −58/−34 region of the AT1R gene promoter in PPARγ-induced AT1R suppression, we hypothesized that the same site may also be important in Tel-induced suppression. The luciferase construct with mutation in GC box (Sp1 site) failed to respond to Tel (Fig. 4A), indicating the important role of Sp1 site in Tel-induced downregulation. In addition, Tel did not affect the degradation rate of AT1R mRNA (Fig. 4B). These data suggested that Tel inhibits AT1R gene transcription and does not affect AT1R mRNA stability.

3.3. Tel-induced AT1R downregulation is PPARγ dependent

To examine the role of PPARγ in Tel-induced AT1R suppression, we examined the effect of GW9662, a PPARγ antagonist. Although GW9662 itself did not affect AT1R expression, preincubation with GW9662 blocked AT1R suppression induced by Tel (Fig. 5).

4. Discussion

In the present study, we demonstrated that Tel, an AT1R antagonist, suppressed the AT1R expression through the PPARγ-mediated pathway. This is the first study that demonstrates the suppression of AT1R expression by AT1R antagonist in VSMCs.

The expression of AT1R was suppressed at both mRNA and protein levels. The results of the promoter assay and the mRNA stability assay suggested that the suppression occurred at the transcriptional level rather than the post-transcriptional level.

The involvement of PPARγ on AT1R suppression was confirmed by experiments using GW9662. GW9662 prevented the Tel-induced suppression of ATR expression, indicating the critical role of PPARγ in this pathway. The ability to activate PPARγ is reported to be unique to Tel and irbesartan (Irb) among several AT1R antagonists [10]. In our study, though we have not examined the effect of Irb, Can (Fig. 3) and Olm (data not shown) had no effect on AT1R expression. Our results seem to be consistent with the previous report [10].

Schupp et al. reported that a subset of AT1R blockers (ARB), Tel and Irb, induced PPARγ activity and promoted PPARγ-dependent differentiation in 3T3-L1 adipocytes [9]. These ARB activated PPARγ by direct interaction with the ligand binding domain (LBD) of PPARγ [9].

The docking studies of the molecular binding model explained the difference in the ability to activate PPARγ among several ARB and full agonists of PPARγ by comparing their interaction with residues of several helixes [10]. According to this model, Tel fits in the LBD of PPARγ surrounded by helixes H3, H6, and H7. However, Tel does not interact with activation function-2 helix that is responsible for receptor activation and stabilization by full PPARγ agonists. Irb, Can, and Olm, so-called tetrazole-containing ARBs, made contact with helix H3 but not H7. The difference in the interaction with these helixes of LBD of PPARγ might contribute to their potential to activate PPARγ.

On activation by a ligand, PPARγ regulates the expression of several genes involved in lipid and carbohydrate metabolism [25,26] and inflammatory responses [27]. From the molecular insight, these effects are basically due to two different transcriptional regulatory mechanisms, one is transactivation and the other is transrepression. Transactivation is dependent on PPARγ response element (PPRE). Upon activation, PPARγ forms a heterodimer with retinoid X receptor and binds to PPRE in the promoter region of the target genes such as CD36 and glucose transporter 4. In contrast, transrepression involves interference with other transcription factors such as NF-κB and AP-1. Because there is no consensus sequence of PPRE in the AT1R gene promoter up to −980 bp, the suppression of AT1R gene transcription should have occurred through the latter mechanism.

This assumption is well substantiated by a previous study which reported that suppression of AT1R gene expression by

PPARγ activation was independent of PPRE [16]. The authors demonstrated that the −58/−34 region of the AT1R gene promoter, including Sp1 binding site, was essential to the PPARγ activator-induced AT1R suppression. They concluded that activated PPARγ inhibited Sp1 function by direct protein–protein interaction. Our study with Tel also demonstrated the essential role of Sp1 binding site in the suppression of AT1R expression. Therefore, Tel may inhibit Sp1 function through the activation of PPARγ resulting in downregulation of the AT1R expression.

Our previous studies showed that downregulation of AT1R by PPARγ activator attenuated cellular response to Ang II [15]. However, Ang II induced ERK activation was almost completely blocked by Tel even at 1 μmol/L, which did not affect AT1R expression because of AT1R blocking effect (Fig. 2C). Therefore, AT1R binding effect is expected at the lower concentration of Tel and dual effect of AT1R binding and AT1R downregulation is expected at higher concentration.

TZDs, synthetic PPARγ activators, are reported to inhibit atherogenesis by regulating various gene expressions. Several studies have demonstrated the anti-atherogenic effects of PPARγ activators in both animal models and human. Rosiglitazone (Rosi), one of TZDs, was shown to have additive effects on plaque regression in the combination treatment with simvastatin in an atherosclerotic rabbit model [28]. Anti-atherogenic effect of Rosi was also reported in a diabetes–atherosclerosis mouse model [29]. AT1R antagonists are reported to suppress atherogenesis. Strawn et al. demonstrated that losartan attenuated atherogenesis in monkeys with hypercholesterolemia [30]. Based on these studies, Tel may be more efficient in suppressing atherosclerotic vascular diseases due to its properties of PPARγ activation and AT1R antagonism.

TZDs are also effective in improving insulin sensitivity and they are already utilized to treat patients with type 2 diabetes [31]. Although the precise mechanism for PPARγ-mediated insulin sensitization is not clear, TZDs reduced fasting and postprandial glucose concentration, and insulin level. Ang II also affects insulin sensitivity [32]. The inhibition of AT1R by losartan improved insulin sensitivity [33] and, in the LIFE study, losartan significantly reduced the incidence of new-onset diabetes in patients with hypertension compared with atenolol [34]. Therefore, the dual effects of Tel may synergistically improve insulin sensitivity.

The dual function of Tel, an AT1R antagonist and a partial agonist of PPARγ, may be quite useful for the treatment of patients with hypertension with complications such as diabetes and atherosclerosis. Considering the blockade of Ang II, the downregulation of AT1R through the activation of PPARγ adds further possibility of Tel. This may result in more complete inhibition of the Ang II. However, it remains to be determined whether Tel suppresses the expression of AT1R in vivo and is superior to other AT1R antagonists in terms of the inhibition of the progression of cardiovascular diseases. Further study is needed.

Acknowledgements

This study was supported in part by grants from Takeda Science Foundation, Kimura Memorial Heart Foundation Research Grant for 2005, and Grants-in-aid for Scientific Research from the Ministry of Education, Culture, Sports, Science and Technology of Japan (17590742) to T.I.

References

[1] de Gasparo M, Catt KJ, Inagami T, Wright JW, Unger T. International union of pharmacology. XXIII. The angiotensin II receptors. Pharmacol Rev 2000;52:415–72.
[2] Brenner BM, Cooper ME, de Zeeuw D, Keane WF, Mitch WE, Parving HH, et al. Effects of losartan on renal and cardiovascular outcomes in patients with type 2 diabetes and nephropathy. N Engl J Med 2001;345:861–9.
[3] Diez J, Querejeta R, Lopez B, Gonzalez A, Larman M, Martinez Ubago JL. Losartan-dependent regression of myocardial fibrosis is associated with reduction of left ventricular chamber stiffness in hypertensive patients. Circulation 2002;105:2512–7.
[4] Scheen AJ. Prevention of type 2 diabetes mellitus through inhibition of the renin–angiotensin system. Drugs 2004;64:2537–65.
[5] Chiu AT, Herblin WF, McCall DE, Ardecky RJ, Carini DJ, Duncia JV, et al. Identification of angiotensin II receptor subtypes. Biochem Biophys Res Commun 1989;165:196–203.
[6] Horiuchi M, Akishita M, Dzau VJ. Recent progress in angiotensin II type 2 receptor research in the cardiovascular system. Hypertension 1999;33:613–21.
[7] Gillespie EL, White CM, Kardas M, Lindberg M, Coleman CI. The impact of ACE inhibitors or angiotensin II type 1 receptor blockers on the development of new-onset type 2 diabetes. Diabetes Care 2005;28:2261–6.
[8] Healey JS, Baranchuk A, Crystal E, Morillo CA, Garfinkle M, Yusuf S, et al. Prevention of atrial fibrillation with angiotensin-converting enzyme inhibitors and angiotensin receptor blockers: a meta-analysis. J Am Coll Cardiol 2005;45:1832–9.
[9] Schupp M, Janke J, Clasen R, Unger T, Kintscher U. Angiotensin type 1 receptor blockers induce peroxisome proliferator-activated receptor-gamma activity. Circulation 2004;109:2054–7.
[10] Benson SC, Pershadsingh HA, Ho CI, Chittiboyina A, Desai P, Pravenec M, et al. Identification of telmisartan as a unique angiotensin II receptor antagonist with selective PPARgamma-modulating activity. Hypertension 2004;43:993–1002.
[11] Yki-Jarvinen H. Thiazolidinediones. N Engl J Med 2004;351:1106–18.
[12] He W, Barak Y, Hevener A, Olson P, Liao D, Le J, et al. Adipose-specific peroxisome proliferator-activated receptor gamma knockout causes insulin resistance in fat and liver but not in muscle. Proc Natl Acad Sci U S A 2003;100:15712–7.
[13] Marx N, Kehrle B, Kohlhammer K, Grub M, Koenig W, Hombach V, et al. PPAR activators as antiinflammatory mediators in human T lymphocytes: implications for atherosclerosis and transplantation-associated arteriosclerosis. Circ Res 2002;90:703–10.
[14] Collins AR, Meehan WP, Kintscher U, Jackson S, Wakino S, Noh G, et al. Troglitazone inhibits formation of early atherosclerotic lesions in diabetic and nondiabetic low density lipoprotein receptor-deficient mice. Arterioscler Thromb Vasc Biol 2001;21:365–71.
[15] Takeda K, Ichiki T, Tokunou T, Funakoshi Y, Iino N, Hirano K, et al. Peroxisome proliferator-activated receptor gamma activators down-regulate angiotensin II type 1 receptor in vascular smooth muscle cells. Circulation 2000;102:1834–9.
[16] Sugawara A, Takeuchi K, Uruno A, Ikeda Y, Arima S, Kudo M, et al. Transcriptional suppression of type 1 angiotensin II receptor gene expression by peroxisome proliferator-activated receptor-gamma in vascular smooth muscle cells. Endocrinology 2001;142:3125–34.

[17] Yang H, Lu D, Raizada MK. Angiotensin II-induced phosphorylation of the AT1 receptor from rat brain neurons. Hypertension 1997;30:351–7.
[18] Gupta M, Miller BA, Ahsan N, Ulsh PJ, Zhang MY, Cheung JY, et al. Expression of angiotensin II type I receptor on erythroid progenitors of patients with post transplant erythrocytosis. Transplantation 2000;70:1188–94.
[19] Chomczynski P, Sacchi N. Single-step method of RNA isolation by acid guanidinium thiocyanate–phenol–chloroform extraction. Anal Biochem 1987;162:156–9.
[20] Takeuchi K, Alexander RW, Nakamura Y, Tsujino T, Murphy TJ. Molecular structure and transcriptional function of the rat vascular AT1a angiotensin receptor gene. Circ Res 1993;73:612–21.
[21] Guo DF, Uno S, Ishihata A, Nakamura N, Inagami T. Identification of a *cis*-acting glucocorticoid responsive element in the rat angiotensin II type 1A promoter. Circ Res 1995;77:249–57.
[22] Sambrook J, Fritsch EF, Maniatis T. Molecular cloning. New York: Cold Spring Harbor Laboratory Press; 1989. p. 16.66–7.
[23] Lin Y, Zhu X, McLntee FL, Xiao H, Zhang J, Fu M, et al. Interferon regulatory factor-1 mediates PPARgamma-induced apoptosis in vascular smooth muscle cells. Arterioscler Thromb Vasc Biol 2004;24:257–63.
[24] Baek SJ, Kim JS, Nixon JB, DiAugustine RP, Eling TE. Expression of NAG-1, a transforming growth factor-beta superfamily member, by troglitazone requires the early growth response gene EGR-1. J Biol Chem 2004;279:6883–92.
[25] Tontonoz P, Hu E, Devine J, Beale EG, Spiegelman BM. PPAR gamma 2 regulates adipose expression of the phosphoenolpyruvate carboxykinase gene. Mol Cell Biol 1995;15:351–7.
[26] Singh Ahuja H, Liu S, Crombie DL, Boehm M, Leibowitz MD, Heyman RA, et al. Differential effects of rexinoids and thiazolidinediones on metabolic gene expression in diabetic rodents. Mol Pharmacol 2001;59:765–73.
[27] Diep QN, El Mabrouk M, Cohn JS, Endemann D, Amiri F, Virdis A, et al. Structure, endothelial function, cell growth, and inflammation in blood vessels of angiotensin II-infused rats: role of peroxisome proliferator-activated receptor-gamma. Circulation 2002;105:2296–302.
[28] Tao L, Liu HR, Gao E, Teng ZP, Lopez BL, Christopher TA, et al. Antioxidative, antinitrative, and vasculoprotective effects of a peroxisome proliferator-activated receptor-gamma agonist in hypercholesterolemia. Circulation 2003;108:2805–11.
[29] Phillips JW, Barringhaus KG, Sanders JM, 0Yang Z, Chen M, Hesselbacher S. Rosiglitazone reduces the accelerated neointima formation after arterial injury in a mouse injury model of type 2 diabetes. Circulation 2003;108:1994–9.
[30] Strawn WB, Chappell MC, Dean RH, Kivlighn S, Ferrario CM. Inhibition of early atherogenesis by losartan in monkeys with diet-induced hypercholesterolemia. Circulation 2000;101:1586–93.
[31] Miyazaki Y, Mahankali A, Matsuda M, Glass L, Mahankali S, Ferrannini E. Improved glycemic control and enhanced insulin sensitivity in type 2 diabetic subjects treated with pioglitazone. Diabetes Care 2001;24:710–9.
[32] Velloso LA, Folli F, Sun XJ, White MF, Saad MJ, Kahn CR. Cross-talk between the insulin and angiotensin signaling systems. Proc Natl Acad Sci U S A 1996;93:12490–5.
[33] Olsen MH, Fossum E, Hoieggen A, Wachtell K, Hjerkinn E, Nesbitt SD. Long-term treatment with losartan versus atenolol improves insulin sensitivity in hypertension: ICARUS, a LIFE substudy. J Hypertens 2005;23:891–8.
[34] Lindholm LH, Ibsen H, Borch-Johnsen K, Olsen MH, Wachtell K, Dahlof B. Risk of new-onset diabetes in the losartan intervention for endpoint reduction in hypertension study. J Hypertens 2002;20:1879–86.

A third-generation, long-acting, dihydropyridine calcium antagonist, azelnidipine, attenuates stent-associated neointimal formation in non-human primates

Kaku Nakano[a], Kensuke Egashira[a], Hideo Tada[a], Yoshiro Kohjimoto[b], Yasuhiko Hirouchi[b], Shun-ichi Kitajima[b], Yasuhisa Endo[c], Xiao-Hang Li[d] and Kenji Sunagawa[a]

Background Calcium antagonists have been shown to reduce atherogenesis and improve clinical outcomes in atherosclerotic vascular disease. No study has so far, however, addressed the effects of calcium antagonists on stent-associated neointimal formation. We therefore investigated whether a third-generation calcium antagonist, azelnidipine, attenuates in-stent neointimal formation in non-human primates.

Method Male cynomolgus monkeys were fed a high cholesterol diet for 4 weeks, and were randomly assigned to three groups: a vehicle group and two other groups treated with azelnidipine at 3 and 10 mg/kg per day for an additional 24 weeks ($n = 12$ each). Multi-link stents were then implanted in the iliac artery.

Results Azelnidipine at the high dose reduced neointimal thickness (0.25 ± 0.02 versus 0.19 ± 0.02 mm; $P < 0.05$). Azelnidipine also reduced local oxidative stress and monocyte chemoattractant protein 1 (MCP-1) expression. No difference was found between the three groups in the degrees of injury score, inflammation score, plaque neovascularization, or plasma lipid levels. Azelnidipine also reduced MCP-1-induced proliferation/migration of vascular smooth muscle cells *in vitro*.

Conclusions This study demonstrated for the first time that azelnidipine attenuates in-stent neointimal formation associated with the reduced expression of MCP-1 and smooth muscle proliferation/migration in the neointima. These data in non-human primates suggest potential clinical benefits of azelnidipine as a 'vasculoprotective calcium antagonist' in patients undergoing vascular interventions. *J Hypertens* 24:1881–1889 © 2006 Lippincott Williams & Wilkins.

Journal of Hypertension 2006, 24:1881–1889

Keywords: monocyte, neointimal hyperplasia, restenosis, smooth muscle cell

[a]Department of Cardiovascular Medicine, Graduate School of Medical Sciences, Kyushu University, Fukuoka, Japan, [b]Primate Research Center, Guandong, China, [c]Department of Applied Biology, Kyoto Institute of Technology, Kyoto, Japan and [d]Gaoyao Kangda Laboratory Animal Science and Technology, Guandong, China

Correspondence and requests for reprints to Kensuke Egashira, MD, PhD, Department of Cardiovascular Medicine, Graduate School of Medical Science, Kyushu University, 3-1-1 Maidashi, Higashi-ku, Fukuoka 812-8582, Japan
Tel: +81 92 642 5358; fax: +81 92 642 5375; e-mail: egashira@cardiol.med.kyushu-u.ac.jp

Sponsorship: This study was supported by grants-in-aid for scientific research (nos. 14657172 and 14207036) from the Ministry of Education, Science, and Culture, Tokyo, Japan, by health science research grants (Comprehensive Research on Aging and Health, and Research on Translational Research) from the Ministry of Health Labor and Welfare, Tokyo, Japan, and by the Program for the Promotion of Fundamental Studies in Health Sciences of the Organization for Pharmaceutical Safety and Research, Tokyo, Japan.

Received 19 September 2005 Revised 10 April 2006
Accepted 12 April 2006

Introduction

Dihydropyridine calcium antagonists have been used worldwide for patients with hypertension and atherosclerotic vascular disease. Recent clinical trials with calcium antagonists provided evidence suggesting that reducing arterial blood pressure close to normal ranges is of great importance in reducing cardiovascular events [1–4]. Notably, in the Comparison of Amlodipine versus Enalapril to Limit Occurences of Thrombosis (CAMELOT) trial [5], compared with placebo and enalapril, the third-generation calcium antagonist amlodipine was shown to reduce hospitalization as a result of unstable angina and revascularization in patients with coronary artery disease already being treated with aspirin, beta-blockers, or statins. These latest clinical trials suggest that there might be pleiotropic actions of calcium antagonists beyond blood pressure lowering. The pleiotropic actions of calcium antagonists may be distinct from pharmacological actions related to L-type calcium channel blockade, but may be attributable to their lipophilic character leading to a high affinity with membrane phospholipid of arterial wall cells such as vascular smooth muscle cells (VSMC) [6]. The vasculoprotective actions of such calcium antagonists include an improvement in endothelial function, an anti-inflammation effect, anti-oxidant function, antiproliferation of VSMC and so forth.

In animal experiments, calcium antagonists have been shown to prevent or attenuate atherosclerosis [7,8], hypertension-induced vascular remodeling [9], heart failure [10] and neointimal formation after balloon injury [11]. However, no study has so far addressed the effects of

calcium antagonists on stent-associated neointimal formation. Investigating this subject must be of clinical importance, because stent implantation is now the major revascularization technique worldwide in patients with atherosclerotic vascular disease. Although a drug-eluting stent reduces the restenosis rate in selected arterial lesions, stent-associated restenosis remains an unsolved clinical issue in high-risk lesions. The cellular mechanism of restenosis after stenting is presumed to be neointimal formation as a result of VSMC proliferation/migration, recruitment of bone marrow-derived progenitor cells or inflammation in response to injury [12–14].

Azelnidipine is a newly developed third-generation calcium antagonist and has antihypertensive action that is comparable to amlodipine [15]. Azelnidipine has strong lipophilicity and affinity to membranes of VSMC [16,17]. Therefore, the aim of this study was to investigate whether azelnidipine at a clinical dose range attenuates in-stent neointimal formation in non-human primates (cynomolgus monkeys). To gain clinical significance for the results obtained, we used a non-human primate model of stent-associated neointimal formation [12].

Materials and methods

Experimental animals

Thirty-six 5-year-old male cynomolgus monkeys weighing 4.2–6.6 kg were purchased. The study protocol was reviewed and approved by the Committee on the Ethics of Animal Experiments, Kyushu University Graduate School of Medical Sciences. The animal care before and after the operation of the animal model was performed in Gaoyao Kangda Laboratory Animal Science and Technology in China. A part of this study was performed at the Station for Collaborative Research and the Morphology Core, Kyushu University Graduate School of Medical Sciences.

Animal model of in-stent restenosis

All animals were fed a high-cholesterol diet (0.5% cholesterol and 6% corn oil) for 4 weeks before stent implantation (Fig. 1). Ticlopidine 100 mg and aspirin 81 mg were started 7 days before the initial procedure. Aspirin was to be given and continued until animals were killed at 6 months, and ticlopidine was administered for 28 days. The animals were randomly assigned to three groups as follows: (i) no treatment vehicle control group (0.5% carboxymethyl cellulose sodium salt); (ii) low-dose azeenidipine (3 mg/kg per day; donated by Sankyo Pharmaceutical Co., Tokyo, Japan) group; (iii) high-dose azelnidipine (10 mg/kg per day) group ($n = 12$ each). Azelnidipine treatment was carried out once a day by gavage for 24 weeks. One week after grouping, all monkeys were anaesthetized with ketamine hydrochloride (10 mg/kg intramuscularly) and sodium pentobarbital (30 mg/kg intravenously), and underwent the placement of a 15 mm-long Multilink stent mounted over the 3-mm balloon implanted in the iliac artery (30 s inflation at 6 atm followed by 60 s inflation at 8 atm, resulting in a stent-to-artery ratio of 1.2 : 1.0) as described [12]. After the operation, all monkeys were fed the same high-cholesterol diet.

Fig. 1

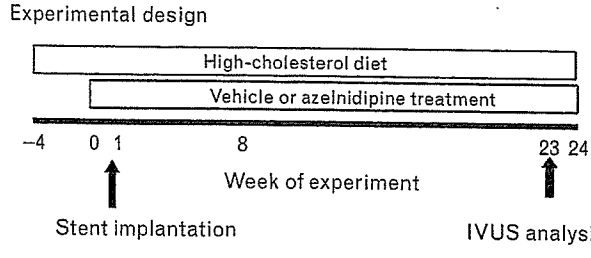

Experimental design. IVUS, Intravascular ultrasound.

Histopathology and immunohistochemistry

Stented arterial sections were excised and fixed for 24 h with 95% ethanol and 1% acetic acid. Each segment was divided into two parts at the centre of the stent. The proximal part was embedded in methyl methacrylate mixed with *n*-butyl methacrylate to allow for sectioning through metal stent struts. Serial sections were stained with elastica van Gieson and haematoxylin eosin. To evaluate the stent area, lumen area, medial area, and neointimal area, the neointimal thickening (neointimal area/length of internal elastica lamina; IEL) were measured. An immunohistochemical study was performed with antibodies against human smooth muscle actin (1A4; Dako, Tokyo, Japan) and von Willebrand factor (vWF; Dako). To evaluate the degree of neovascularization the number of arterioles in the intima and adventitia were counted.

The distal part was used for immunohistochemical analysis. After stent struts were gently removed with micro forceps, the tissue was dehydrated, embedded in paraffin, and cut into 5-μm thick slices. They were subjected to immunostaining using antibodies against human monocyte chemoattractant protein 1 (MCP-1; Santa Cruz, California, USA) and C-C chemokine receptor 2 (CCR2, Santa Cruz) as described [12]. A single observer, who was blinded to the experiment protocol, performed the morphometry. All images were captured by an Olympus microscope equipped with a digital camera (HC-2500) and were analysed using Adobe Photoshop 6.0 (Adobe Systems, San Jose, California, USA) and Scion Image 1.62 (Scion, Frederick, Maryland, USA) software.

Local oxidative stress with fluorescent dihydroethidium micrographic analysis

Frozen, enzymatically intact, sections (10-μm thick) just at the proximal edge of stented iliac arteries were incubated with dihydroethidium (10 μmol/l; Sigma, Tokyo,

Japan) in phosphate-buffered saline for 30 min at 37°C in a humidified chamber protected from light. Ethidium bromide was detected by fluorescent microscopy as described previously [18]. One representative section per artery was counted in all animals.

Intravascular ultrasound procedure and analysis

Twenty-three weeks after stent implantation, intravascular ultrasound imaging (IVUS) was performed. The imaging was performed using a 40 MHz ultrasonic imaging catheter (Ultra Cross; Boston Scientific, Boston, Massachusetts, USA) and an automatic pullback device, and the studies were recorded on 1/2-inch high-resolution s-VHS tapes for off-line volumetric assessment. IVUS analysis included stent area and proliferative intimal area.

Injury and inflammation scores

The injury and inflammatory scores were determined at each strut site, and mean values were calculated for each stented segment as previously described [19,20]. In brief, a numeric value from 0 (no injury) to 3 (most injury) was assigned: 0, endothelial denudate, IEL intact; 1, IEL lacerated, media compressed, not lacerated; 2, IEL lacerated, media lacerated, external elastica lamina compressed, not lacerated; and 3, media severely lacerated, external elastica lamina lacerated, adventitia may contain stent strut. The average injury score for each segment was calculated by dividing the sum of injury scores by the total number of struts at the examined section. The inflammation score took into consideration the extent and density of the inflammatory infiltrate in each individual strut. With regard to the inflammatory score for each individual strut, the grading is: 0, no inflammatory cells surrounding the strut; 1, light, non-circumferential inflammatory cells infiltrate surrounding the strut; 2, localized, moderate-to-dense cellular aggregate surrounding the strut non-circumferentially; and 3, circumferential dense inflammatory cells, infiltration of the strut. The inflammatory score for each cross section was calculated in the same manner as for the injury score (sum of the individual inflammatory scores, divided by the number of struts in the examined section).

Biochemical measurements

Biochemical parameters listed in Tables 1 and 2 were measured. MCP-1, interleukin (IL)-8, and transforming growth factor beta 1 were measured using commercially available enzyme-linked immunosorbent assay kits for humans (Quantikine R&D Systems, Minneapolis, Minnesota, USA). 8-Iso prostaglandin F2α (isoprostanes) in the urine was measured by high-performance liquid chromatography/tandem mass spectrometry as previously reported [21]. Isoprostanes were adjusted according to the creatinine level. Urine was collected over 3 h while each animal was in a metabolic cage.

Proliferation and migration assay in vascular smooth muscle cells

Human coronary artery VSMC (Cambrex Bio Science Walkersville Inc., Walkersville, Tennessee, USA) were

Table 1 Systemic biochemical parameters and body weight

		Week of experiment			
Parameters	Groups	0	8	16	24
Total cholesterol (mg/dl)	Vehicle control	430 ± 51	495 ± 51	417 ± 34	646 ± 55*
	Azel 3 mg/kg	470 ± 32	555 ± 62	524 ± 70	631 ± 42*
	Azel 10 mg/kg	437 ± 33	480 ± 47	347 ± 28	568 ± 50*
HDL-cholesterol (mg/dl)	Vehicle control	20 ± 2	19 ± 4	22 ± 6	14 ± 2
	Azel 3 mg/kg	18 ± 2	14 ± 2	15 ± 2	15 ± 2
	Azel 10 mg/kg	21 ± 4	14 ± 2	17 ± 4	16 ± 2
LDL-cholesterol (mg/dl)	Vehicle control	370 ± 46	387 ± 37	315 ± 28	512 ± 39*
	Azel 3 mg/kg	381 ± 31	430 ± 46	385 ± 46	466 ± 27*
	Azel 10 mg/kg	298 ± 32	381 ± 40	267 ± 24	420 ± 29*
Triglycerides (mg/dl)	Vehicle control	16 ± 3	16 ± 4	13 ± 1	18 ± 2
	Azel 3 mg/kg	10 ± 1	16 ± 3	13 ± 2	33 ± 9
	Azel 10 mg/kg	14 ± 1	25 ± 12	12 ± 2	25 ± 4
Glucose (mg/dl)	Vehicle control	58 ± 3	67 ± 3	64 ± 2	62 ± 3
	Azel 3 mg/kg	60 ± 4	60 ± 3	63 ± 3	66 ± 3
	Azel 10 mg/kg	65 ± 4	65 ± 3	61 ± 2	59 ± 3
GOT (unit/l)	Vehicle control	52 ± 6	44 ± 6	50 ± 4	54 ± 4
	Azel 3 mg/kg	51 ± 3	43 ± 3	47 ± 4	55 ± 3
	Azel 10 mg/kg	45 ± 4	41 ± 4	50 ± 6	61 ± 6
GPT (unit/l)	Vehicle control	29 ± 7	21 ± 3	20 ± 4	23 ± 2
	Azel 3 mg/kg	25 ± 2	20 ± 2	22 ± 7	23 ± 2
	Azel 10 mg/kg	21 ± 2	17 ± 2	17 ± 5	28 ± 6
Angiotensin II (pg/ml)	Vehicle control	29 ± 8	19 ± 4	14 ± 2	43 ± 10
	Azel 3 mg/kg	12 ± 2	15 ± 3	15 ± 3	21 ± 5
	Azel 10 mg/kg	12 ± 1	11 ± 2	15 ± 3	31 ± 8
Body weight (kg)	Vehicle control	5.2 ± 0.2	5.6 ± 0.2	6.1 ± 0.2	6.1 ± 0.2
	Azel 3 mg/kg	5.2 ± 0.2	5.6 ± 0.3	5.8 ± 0.3	5.8 ± 0.3
	Azel 10 mg/kg	5.2 ± 0.2	5.6 ± 0.2	6.0 ± 0.3	5.9 ± 0.3

Azel, azelnidipine; GOT, glutamic-oxaloacetic transaminase; GPT, glutamic-pyruvic transaminase; HDL, high-density lipoprotein; LDL, low-density lipoprotein. Data are mean ± SEM ($n = 12$ each). *$P < 0.05$ versus 0 week.

Table 2 Systemic oxidative stress marker and cytokines

Parameters	Groups	Week of experiment			
		0	8	16	24
8-Iso-prostaglandin in urine (ng/mg creatinine)	No treatment	716 ± 86	691 ± 94	654 ± 75	603 ± 88
	Azel 3 mg/kg	714 ± 78	572 ± 92	621 ± 86	626 ± 66
	Azel 10 mg/kg	845 ± 79	674 ± 98	693 ± 92	573 ± 78*
MCP-1 in serum (pg/ml)	No treatment	44 ± 5	40 ± 11	51 ± 3	61 ± 5*
	Azel 3 mg/kg	46 ± 3	37 ± 8	45 ± 3	47 ± 5
	Azel 10 mg/kg	47 ± 4	32 ± 7	29 ± 5†,*	37 ± 4†,*
IL-8 in serum (ng/ml)	No treatment	3.0 ± 0.3	3.8 ± 0.5	4.4 ± 0.5	3.2 ± 0.5
	Azel 3 mg/kg	2.2 ± 0.3	2.9 ± 0.3	4.6 ± 0.4	3.6 ± 0.7
	Azel 10 mg/kg	2.7 ± 0.3	3.3 ± 0.4	4.2 ± 0.8	2.7 ± 0.6
TGF-β1 in serum (ng/ml)	No treatment	63 ± 6	70 ± 7	67 ± 7	47 ± 4
	Azel 3 mg/kg	55 ± 4	67 ± 3	68 ± 7	43 ± 5
	Azel 10 mg/kg	56 ± 4	73 ± 4	62 ± 4	42 ± 3

Azel, azelnidipine; IL, interleukin; MCP-1, Monocyte chemoattractant protein 1; TGF-β1, transforming growth factor beta 1. Data are mean ± SEM ($n = 12$ each). *$P < 0.01$ versus 0 week, †$P < 0.05$ versus no treatment group.

cultured, and placed into 48-well culture plates (Falcon 354506 Biocoat. Cell Ware Human Fibronectin; Bioscience Inc., Bedford Massachusetts, USA). Proliferation was stimulated by human MCP-1 at 10 ng/ml (Sigma). Azelnidipine at 1, 10, and 100 nmol or solvent were added to the wells. Four days later, the cells were fixed with methanol and a single observer, who was blinded to the experimental protocol, counted the number of cells per plate.

The migration of rat aortic smooth muscle cells was assessed with a Boyden chamber type cell migration assay kit housing a collagen-precoated polycarbonate membrane with 8.0-μm pores (Chemicon International Inc., Termacula, California, USA), as previously described [22]. The lower chambers were filled with or without human MCP-1 at 10 ng/ml (Sigma). Then cells (1×10^5 cells/ml) were placed on the upper side of the membrane and allowed to migrate through the pores. After 4 h of incubation, the number of cells that migrated to the lower surface of the membrane was counted per ×200 high-power fields. Azelnidipine at 1, 10, and 100 nmol or solvent was added to the lower chamber.

The concentrations of azelnidipine at ranges of 1–10 nmol can be considered as a clinically relevant dose, because the concentrations are nearly equivalent to the concentration reported in human subjects who were orally administered a 5 or 15 mg azelnidipine tablet [23].

Measurements of arterial blood pressure, heart rate, and plasma azelnidipine levels

Separate preliminary experiments were performed to determine the effects of azelnidipine on arterial blood pressure and heart rate in cynomolgus monkeys under conscious conditions. On the last day of the drug treatment period, blood samples were drawn before and after drug administration, and the plasma drug concentration was determined by gas chromatography–mass spectrometry [15].

Statistical analysis

Data are expressed as the mean ± SE. Statistical analysis of differences was compared by analysis of variance and Dunnet's multiple comparison tests. A P value of less than 0.05 was considered to be statistically significant.

Results

General status

No animals showed any adverse clinical signs (decreased spontaneous motor action, decreased food consumption, diarrhoea, limping and prone position, etc.) during the experimental period and all survived. There was no significant treatment effect on body weight among the groups (Table 1).

Histopathological and immunohistochemical analysis, and detection of local oxidative stress

There were no significant differences in stent area, IEL length, and medial area among all three groups (Fig. 2). Azelnidipine at the high dose tended to decrease the neointimal area (vehicle group, 2.4 ± 0.2; low-dose group, 2.3 ± 0.2; high-dose group, 1.8 ± 0.2 mm^2; vehicle versus high dose $P = 0.07$) and significantly decreased neointimal thickening (vehicle group, 0.25 ± 0.02; low-dose group, 0.24 ± 0.02; high-dose group, 0.19 ± 0.02; vehicle versus high dose $P < 0.05$; Fig. 2).

Both MCP-1 and CCR2 immunoreactivity was not detected in the non-stented normal artery (data not shown). In contrast, intense MCP-1 and CCR2 immunoreactivity was evident in the neointima and media of stented arteries from the control group. The percentage of MCP-1-positive cells in the neointima decreased in the high-dose azelnidipine group (Fig. 3), whereas the percentage of CCR2-positive cells did not differ among the three groups. In contrast, there was no significant difference in the percentage of MCP-1 or CCR2-positive cells in the media among the three groups.

Local oxidative stress was measured with dihydroethidium staining. No apparent dihydroethidium fluorescence

Fig. 2

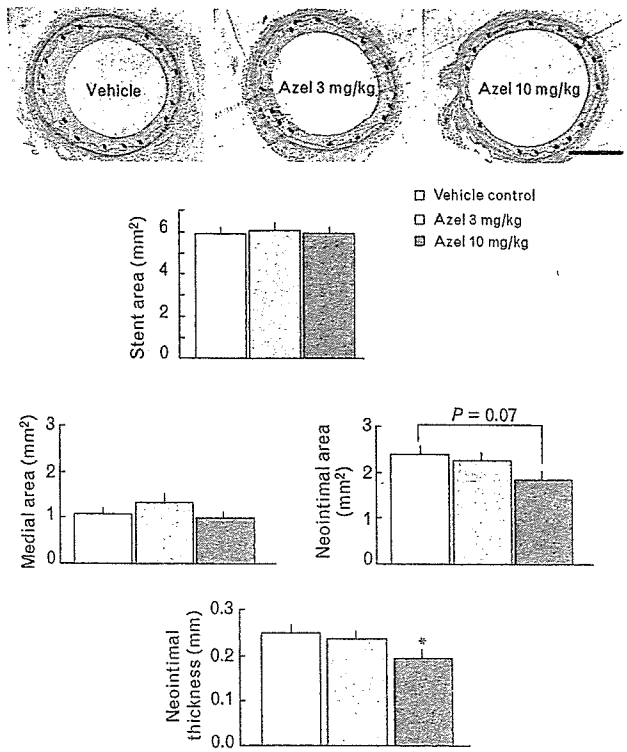

Effects of azelnidipine on stent-associated neointimal formation (histopathological analysis). (a) Representative photomicrographs of cross-sections of the stented iliac artery stained with elastica van Gieson from vehicle control group (left panel), low-dose azelnidipine (Azel) group (middle panel), and high-dose azelnidipine group (right panel) 24 weeks after stenting. Bar 1 mm. (b) Stent area (area within the stent itself), medial area (area within the external elastica lamina minus internal elastica lamina area), neointimal area (area within the internal elastica lamina minus lumen area), and neointimal thickening ($n = 12$ each). $^*P < 0.05$ versus vehicle group. Each value represents mean ± SEM.

Fig. 3

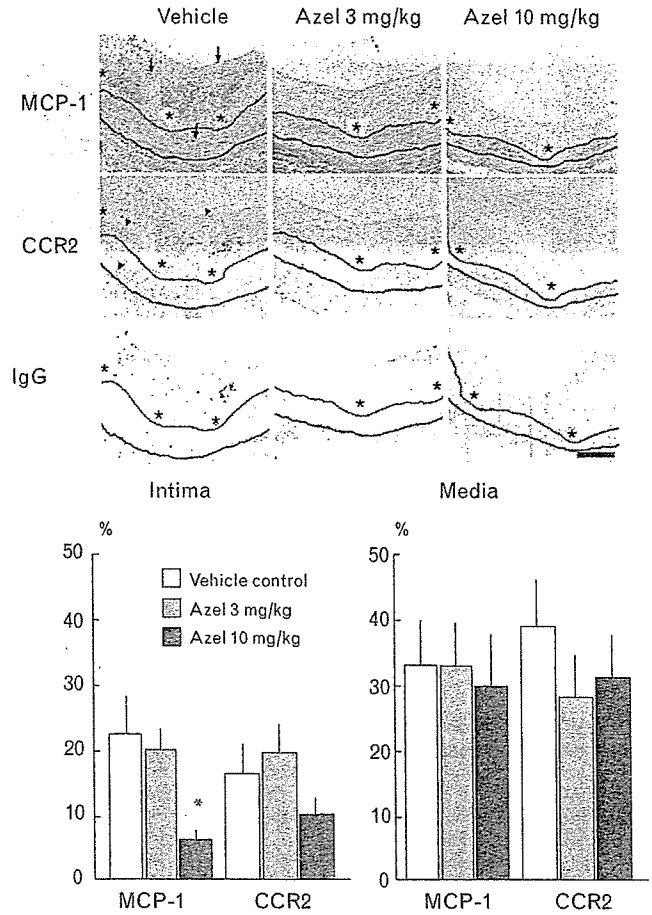

Effects of azelnidipine (Azel) on immunoreactivity for monocyte chemoattractant protein 1 (MCP-1) and C-C chemokine receptor 2 (CCR2). (a) Cross-sections of stented arteries from experimental groups stained immunohistochemically with the antibody against MCP-1 (arrows), CCR2 (arrow heads) or non-immune IgG (* indicates stent strut sites). White and blue lines show internal and external elastica lamina, respectively. (b) The percentages of MCP-1 and CCR2-positive cells in the neointima and media ($n = 12$ each). Bar 100 μm. $^*P < 0.05$ versus vehicle group. Each value represents mean ± SEM.

was detected in the non-stented normal artery (data not shown). As shown in Fig. 4, the fluorescent signal attributable to superoxide production was markedly enhanced in the neointima and media from the control group. The intensity of dihydroethidium fluorescence in the neointima decreased in the high-dose azelnidipine group, whereas the dihydroethidium signal in the media did not differ among the three groups (Fig. 4).

Injury score, inflammation score, and neovascularization

There was no significant difference in the injury score and inflammation score between the three groups (Fig. 5). Also, there were no significant differences in the degrees of neovascularization in the neointima (vWF-positive microvessels/mm^2) and adventitia (vWF-positive microvessels/section; Fig. 5).

Intravascular ultrasound imaging analysis

The degrees of neointimal formation were also investigated by IVUS analysis. As shown in histopathological analysis, high-dose azelnidipine reduced stent-associated neointimal formation by 42% (Fig. 6).

Systemic biochemical parameters

Low and high doses of azelnidipine also did not affect lipid profiles, angiotensin II and liver transaminases (Table 1). Azelnidipine at the high dose decreased 8-iso-prostaglandin F2α in urine at week 24 (Table 2). Serum levels of MCP-1 increased at week 24 in the vehicle group (Table 2). No increase in serum MCP-1 levels was noted in azelnidipine treatment groups. Notably, azelnidipine at the high dose reduced serum MCP-1 levels. In contrast, there were no treatment effects of azelnidipine on serum levels of IL-8 and transforming growth factor beta 1 (Table 2).

Fig. 4

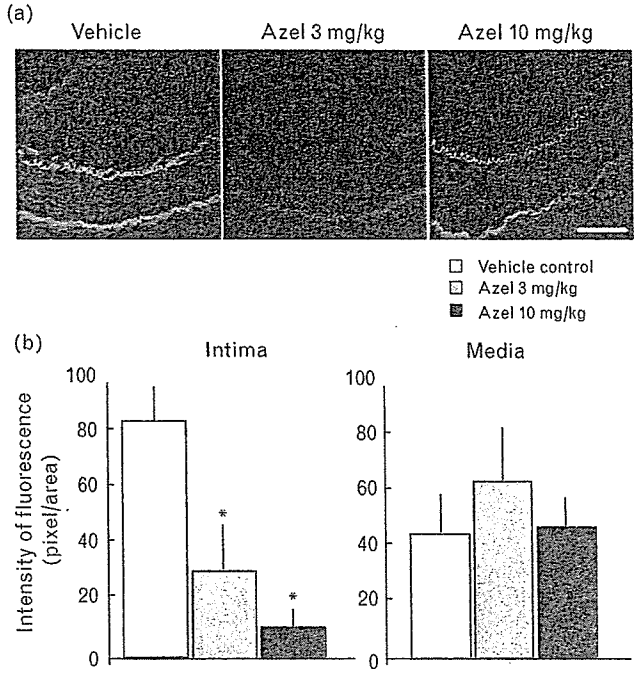

Effects of azelnidipine (Azel) on local oxidative stress marker. (a) Representative superoxide detection with dihydroethidium in cross-sections of iliac arteries. Red colour expressed dihydroethidium-stained positive nuclei, and yellow or green expressed autofluorescences. Autofluorescences were agreed internal elastica lamina (upper line) and external elastica lamina (lower line). Bar 100 μm. (b) Mean fluorescent intensity in the neointima and media ($n = 12$ each). *$P < 0.01$ versus vehicle group. Each value represents mean ± SEM.

Fig. 5

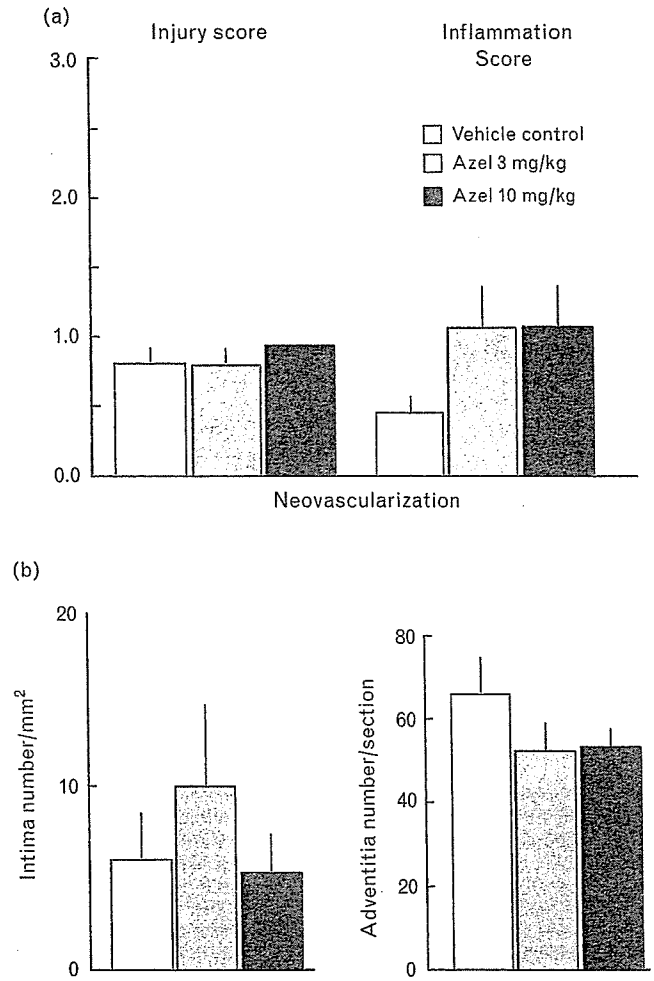

Effects of azelnidipine (Azel) on injury score, inflammation score, and neovascularization. (a) Injury score and inflammation score. (b) The degrees of neovascularization in the neointima and adventitia. The neovascularization were defined as von Willebrand factor (vWF)-positive microvessels/mm^2 in the neointima and vWF-positive microvessels/section in adventitia ($n = 12$ each). Each value represents mean ± SEM.

Proliferation and migration assay of vascular smooth muscle cells

Azelnidipine at 1, 10, and 100 nmol significantly inhibited MCP-1-induced proliferation in a dose-dependent manner (Fig. 7). Azelnidipine also reduced the MCP-1-induced migration of rat aortic smooth muscle cells (Fig. 7).

Haemodynamic parameters and plasma azelnidipine concentrations

Azelnidipine at the low and high doses did not affect haemodynamic parameters (Table 3). The maximum concentration (C_{max}) of azelnidipine at 3 and 10 mg/kg per day was 36 ± 17 and 107 ± 17 ng/ml, respectively, in monkeys. The C_{max} after oral administration of azelnidipine at 16 mg in hypertensive individuals is reported to be 48 ± 19 ng/ml [15].

Discussion

The present study demonstrated for the first time that a newly developed calcium antagonist, azelnidipine, at 10 mg/kg attenuated neointimal formation 6 months after stent implantation in hypercholesterolemic non-human primates (cynomolgus monkeys). We evaluated the degrees of stent-associated neointimal formation in two ways: histopathological and IVUS analyses. Both methods demonstrated significant benefits of azelnidipine by reducing neointimal formation after stent implantation. Although an appropriate animal model for the evaluation of stent-associated neointimal formation (restenotic changes) is uncertain, the non-human primate model may gain the advantage over non-primate animal models such as rabbits and pigs, because adequate degrees of neointima develop after stenting, and vascular inflammatory and proliferative responses to injury in non-human primates are presumed to be closer to those in humans than other non-primate models. Therefore, the use of non-human primates may allow us to evaluate the efficacy of any therapies on